Chapter1

Introduction

1.1 Background

Due to the high mobility and the capability of realizing integrated circuits on glass, Low temperature polycrystalline silicon (LTPS) thin film transistors (TFTs) have become increasingly important for active-matrix liquid-crystal display (AMLCD) applications such as high-definition television, portable devices, and projection displays. There's several groups focus their attentions on the photo-leakage current, because when LTPS TFTs are applied to projectors, the high illumination intensity increases the leakage current of LTPS TFTs and results in the decrease of pixel voltage and the increase of cross talk. In order to compensate this disadvantage, the behavior of LTPS TFTs under illumination should be figured out.

Reduction of power consumption through backlight control is another important requirement for these applications, one way to achieve this is by sensing the ambient light and then adjust the backlight strength to fit our demands. Therefore, if we integrate the ambient light sensor with the same LTPS technology used to fabricate the display, the fabrication cost can be reduced, and the process can be simplified. Thus in this work we try to summarize the characteristics of photo-leakage current for the purpose of light sensing.

1.2 Studies on Leakage Current of LTPS TFTs

The studies of photo-leakage current should be based on the comprehension of leakage current of LTPS TFTs. Thus understanding of leakage current mechanism is

necessary.

1.2.1 Review of Leakage Current Mechanism

It has been confirmed that leakage current occurs near the drain depletion region, thus the conduction of the leakage current is determined by the applied voltage across the depletion region. Reports revealed that the conduction mechanism consist of several processes [1, 2]. When a low drain bias apply, the activation energy is large, which indicate that for a carrier emitted from the trap to conduction band must overcome a large energy barrier. Thermionic emission is the dominant leakage mechanism at low field. As drain bias increases, the drain depletion field increases while the activation energy decreases, which means the barrier that carriers have to overcome is lowering. As such, the dominant leakage mechanism is thermionic field emission. This process could be accomplished by combination of thermionic emission and tunneling processes. Further increase of the drain field, while the activation energy is put below 0.1eV, the dominant leakage mechanism is tunneling. Fig. 1-1 shows the schematic illustration of the leakage mechanism model.

From the description above, we can summarize that the transport of carriers was decided by the kinetic energy afforded either by thermal energy or by electric field, and trap states in the band gap act as a bridge for the conduction. Thus we know that most decisive factors of leakage current are temperature, bias, and trap state distribution. Therefore, we suspect the photo leakage current may also have strong dependence on these parameters.

1.2.2 Studies on Photo Leakage Current

To the best of our knowledge, Almost all the studies about photo effects in poly-si TFTs pay their attentions on the off-condition of TFTs, i.e. the photo leakage current. Fig. 1-2 shows the IV curve with and without illumination. It's obviously

noticed that the leakage current arises about 1~3 orders under illumination. Refers to the on-region and sub threshold-region, photo effect is relatively weak.

Kobayashi et al [3]. demonstrated that the photo-leakage current occurs in the drain depletion region as well as the leakage current does. It indicated that photo leakage current is proportional to channel width, and independent of channel length unless the length is smaller than 2.5 μm, where short-channel effect may affect photo leakage current.

The effect of LDD length and the dopant concentration is also significant. The relationship between photo current and LDD length is almost linear, and when LDD length = 0.8 μm, photo current increases with the dopant concentration; while LDD length = 3.9 μm, photo current decreases when the dopant concentration increases.

Suzuki et al [4]. found that under backlight illumination, the photo leakage current has strong dependence with the poly-si thin film thickness. They also modeled the phenomena by assuming that the electron-hole pairs generate and recombine at both interfaces of poly-si thin film.

1.3 Motivation

However, under the consideration of applying LTPS TFTs on light sensing, we surely need more knowledge about the physical mechanism of photo leakage current. As the paragraph above mentioned, we expect that temperature, electric filed, and the defect states in the poly-si thin film may be the major influence on the photo leakage current. We would like to find the way to “predict” the photo leakage current behavior under certain conditions before illumination. Then, it will be convenient to choose the operating condition when LTPS TFTs were applied on sensing. On the other hand, we hope to construct an explanation to describe how the current is generated and varies

under different temperatures, bias conditions, even for different defect distribution.

1.4 Thesis Organization

Chapter 1 Introduction

1.1 Background

1.2 Studies on Leakage Current of Poly-Si TFT

1.2.1 Review of Leakage Current Mechanism

1.2.2 Studies on Photo Leakage Current

1.3 Motivation

1.4 Thesis Organization

Chapter 2 Experiments

2.1 Device Fabrication

2.2 Experiment Method

2.3 Parameter Extraction Method

Chapter 3 Characteristics of Photo Leakage Current

3.1 Discussion of $R_{L/D}$

3.2 Definition of Unit-Lux Current

3.3 Field Effect on Unit-Lux Current

3.3.1 Drain Bias Effect on Unit-Lux Current

3.3.2 Gate Bias Effect on Unit-Lux Current

3.3.3 Anaysis of Unit-Lux Current

3.4 Temperature Effect on Unit-Lux Current

3.5 Device Variation of Unit-Lux Current

Chapter 4 Photo Leakage Current after Extra Defect Creation

4.1 Extra Defect Creation after Hot Carrier Stress

4.1.1. Degradation Mechanism and Stress Condition

4.1.2. Photo Leakage Current Variation after Stress

4.1.3. Comparison between Unit-Lux Current Variation and Device Parameters

4.1.4. ULC under Different VD, VG Conditions

4.2 Extra Defect Creation after Self Heating Stress

4.2.1. Degradation Mechanism and Stress Condition.

4.2.2. Photo Leakage Current Variation after Stress.

4.2.3. Comparison between Unit-Lux Current Variation and Device Parameters

4.2.4. ULC under Different VD, VG Conditions

4.3 Discussion of Carrier Recombination Process

Chapter 5 Conclusions

References

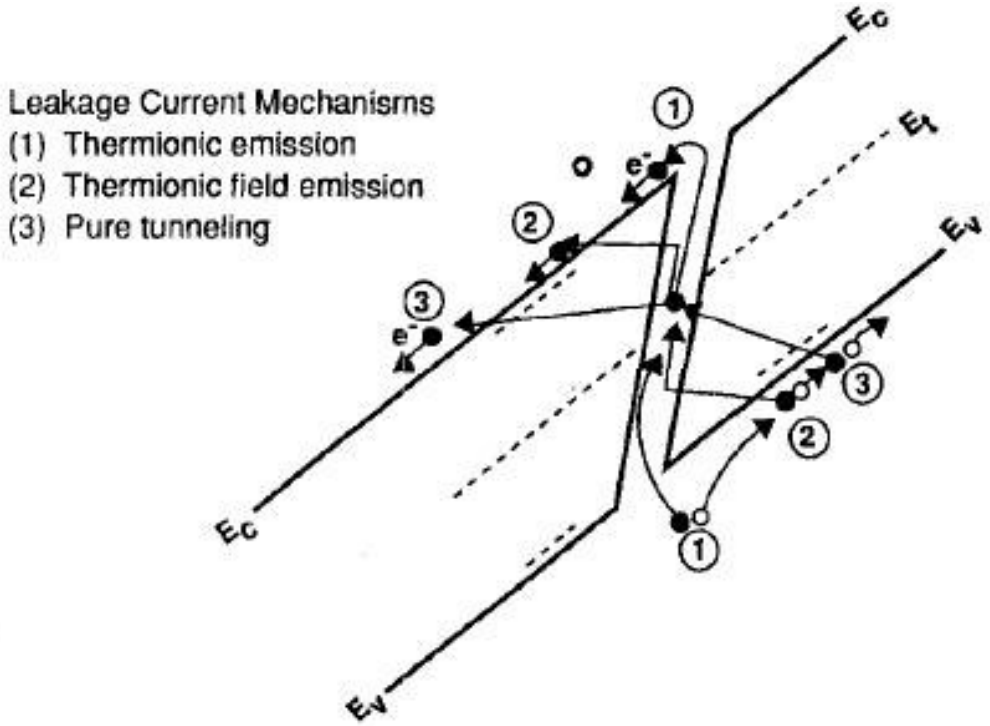

Fig.1-1 Conduction process of leakage current.

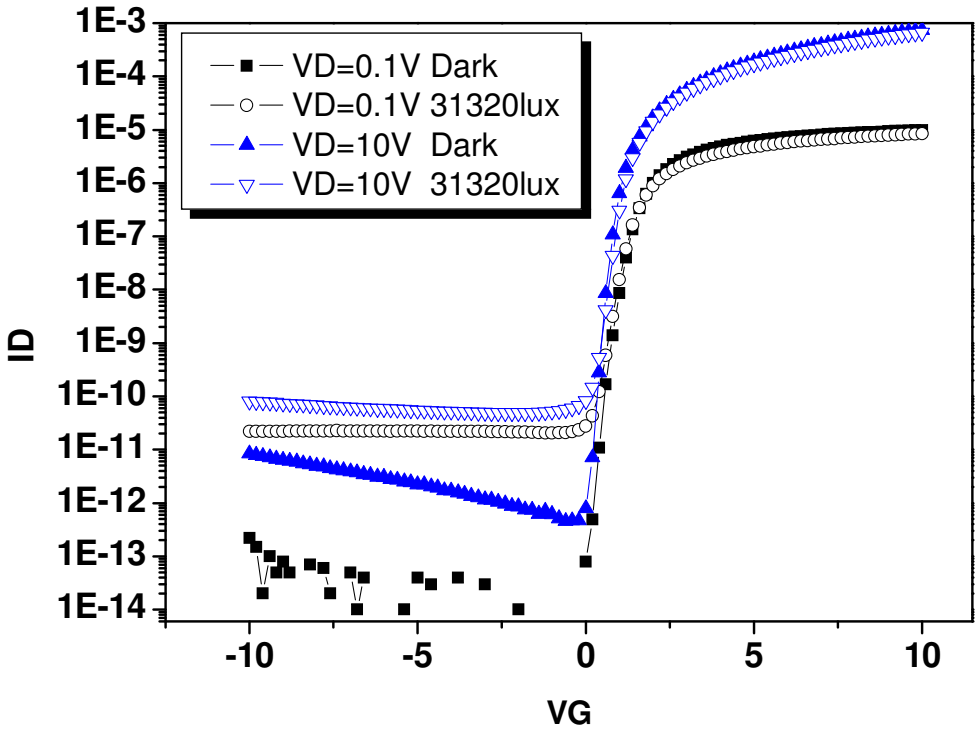

Fig. 1-2 IV curves under 31320 lux illumination.

Chapter2

Experiments

2.1 Device Fabrication

In this experiment, the device we used were the conventional top-gate structure n-channel LTPS TFTs. The cross-section views of n-channel LTPS TFTs are shown in Fig. 2-1. The process flow of TFTs is described as follows: First, the buffer oxide and 50 nm thick a-Si:H films were deposited on glass substrates with plasma-enhanced chemical vapor deposition (PECVD). The samples were then put into the oven for dehydrogenation. The XeCl excimer laser of wavelength 308 nm and energy density of 400 mJ/cm^2 was used to recrystallize the a-Si:H film to poly-Si. After poly-Si active area definition, 65nm gate insulator was deposited with PECVD. Next, the metal gate was formed by sputter and then defined. The lightly doped drain (LDD) and the n+ source/drain doping were formed by PH3 implantation with dosage 2×10^{13} and 2×10^{15} cm^2 of PH_3, respectively. The LDD implantation was self-aligned and the n+ regions were defined with a separate mask. Then the interlayer of SiN_X was deposited. Subsequently, the rapid thermal annealing was conducted to activate the dopants. Meanwhile, the poly-Si film was hydrogenated. Finally, the contact holes formation and metallization were performed to complete the fabrication work. The channel width of TFTs is 20 μm and channel length is 5 μm, while the length of the LDD region is 2.5 μm.

2.2 Experiment Method

In our experiment, the current-voltage characteristic of LTPS TFTs was

measured by HP 4156A semiconductor parameter analyzer. We had focused our attention on the leakage current in the off-region under illumination. Photo leakage current was induced by a halogen lamp irradiation stream with several intensities through the objective of a microscope, and the light intensity was measured by a digital luminous flux meter.

DC stress is performed for extra defect creation. In this article we utilize two different stress conditions for analysis. One of them is Hot Carrier stress which is performed under VG = 3V, VD = 16V. Another is Self Heating stress and the bias condition is VG = VD =15V. In addition, stress times are 1、5、25、100、500、1000 second for different level degradation.

2.3 Parameter Extraction Method

The methods of the typical electrical parameter extraction will be introduced in the following, including threshold voltage, field-effect mobility, subthreshold swing, on-current, and leakage current.

Determination of the Threshold Voltage (V_{th})

The method to determine the threshold voltage in this thesis is the constant drain current method, which is adopted in most studies of TFTs. The threshold voltage is defined as the gate voltage which yields a normalized drain current (i.e. the threshold current). Typically, the threshold current is specified as 10nA at $|V_{ds}|$=0.1V and 100nA at $|V_{ds}|$=10V.

Determination of the Field Effect Mobility (μFE)

The field effect mobility (μ_{EF}) is determined from the transconductance gm at low drain bias. The transfer characteristics of poly-Si TFTs can be derived by a gradual channel approximation. The relation can be expressed as

$$I_d = \mu_{FE} C_{ox} \frac{W}{L}[(V_{gs} - V_{th})V_d - \frac{1}{2}V_d{}^2]$$

Where

C*ox* is the gate oxide capacitance per unit area,

W is channel width,

L is channel length, and

V*th* is the threshold voltage.

The transconductance is defined as

$$g_m = \left.\frac{\partial Id}{\partial Vg}\right|_{Vd=const.} = \mu_{FE} \frac{W}{L} C_{ox} V_d \qquad (2.5)$$

Therefore, the field effect mobility can be obtained by

$$\mu_{FE} = \frac{L}{C_{ox} W V_d} g_m$$

Determination of the Subthreshold Swing (SS)

Subthreshold swing is a measure of the efficacy of the gate potential to modulate drain current. It is defined as the amount of gate voltage to increase and/or decrease drain current by one order of magnitude. It can be shown that the expression for *SS* is given by

$$SS = \frac{\partial V_g}{\partial(\log I_d)}$$

Clearly, the smaller value of *SS*, the better transistor is as a switch. A small value of *SS* means that a small change in the input bias can modulate the output current considerably.

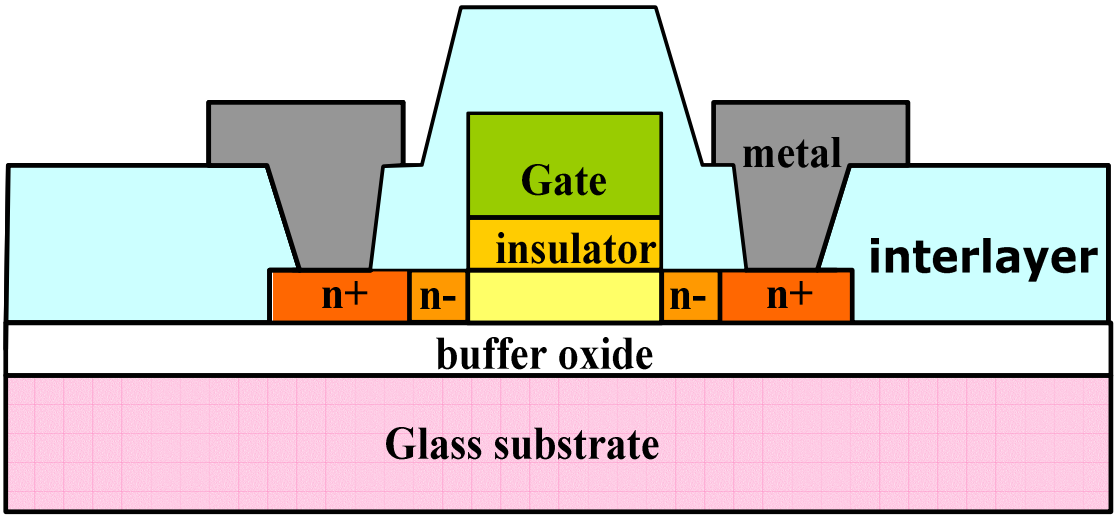

Fig. 2-1 The cross-section views of n-channel LTPS TFTs with LDD structure

Chapter3

Characteristics of Photo Leakage Current

3.1 Discussion of $R_{L/D}$

Fig. 3-1(a) shows the IDVG curve in the saturation region (VD = 10V) and Fig. 3-1(b) shows the IDVD curve in the off region (VG = -5V) under illumination. It's obvious that the drain current measured in the off-condition was lifted up to different levels under different illumination intensities. In this thesis, we regard that the total leakage current under illumination is composed of two major components: One is the leakage current that is not caused by photo illumination, i.e. "*Dark current (Idark)*" which is measured under dark state; the other part is "*Photo leakage current (Iphoto)*" which means the component induced utterly by illumination. Therefore, "photo leakage current" is defined to be the difference between the total leakage current under illumination (Iillum) and dark current (Idark).

For the application of light sensing, previous study [5] has defined an index "$R_{L/D}$" for discussing photo effect of TFTs. $R_{L/D}$ is defined as the ratio between the drain current measured under illumination (Iillum) and Idark. The physical meaning of it is the sensitivity of the induced photo leakage current.

Experiments that we have performed for comparing drain and gate bias effects on photo leakage current are listed in Table 3-1 .The dependences of $R_{L/D}$ on VD, VG biases are shown in Fig. 3-2(a) and Fig. 3-2(b). We can see that $R_{L/D}$ decreases when drain bias increases or gate bias goes more negative. It means the sensitivity of the leakage current would reduce while the voltage difference between drain and gate electrode increases. It is because that large VDG increases Idark more rapidly rather

than Iillum, as shown in Fig. 3-3(a) and Fig. 3-3(b). In contrast to Idark, the dependence of Iillum on VD and VG is nearly constant. Thus the weight of Idark in the total leakage current rises quickly when large VD and VG biases are applied and results in $R_{L/D}$ drops down. Due to the dependence of Iillum on VD and VG is rather weak than Idark, we regard Iillum as constant when extracting $R_{L/D}$. Thus, we can find that the dependence of $R_{L/D}$ on VD and VG is very similar to the reciprocal of Idark.

Therefore, from these plots and discussions, we can conclude that $R_{L/D}$ reflects the variation behavior of dark current, which is not our concern in this thesis. We would only pay attentions on the photo leakage current (Iphoto) behavior in the following sections.

3.2 Definition of Unit-Lux Current

Fig. 3-4 shows the relationship between photo leakage current and illumination intensity, which indicates that they have good linear dependence between each other. Later, we will show that whether the measure condition is, this good linearity is always tenable in the off region, and the only variety is that the slope would be different when we change our measure conditions like drain, gate bias, temperature or different defect distribution. Thus, we define this slope as Unit-Lux Current, (ULC in abbreviation.) which is an important index for discussing the variety of photo leakage current. The physical meaning of Unit-Lux Current is the photo leakage current induced “per unit-photo flux”.

3.3 Field Effect on Unit-Lux Current

3.3.1 Drain Bias Effect on Unit-Lux Current

Relationship between Iphoto and illumination intensity under different drain

biases is shown in Fig. 3-5. It indicates that the linearity has retained but the slope changes when the bias condition changes. Fig. 3-5(a) is obtained by measure photo leakage current at fixed gate bias and several drain biases. It demonstrates that Unit-Lux Current increases significantly while drain bias increases. Fig. 3-5(b) shows how Unit-Lux Current enlarges with drain bias under different gate biases. We've noticed that drain bias affects the photo leakage current in an anomalous way, and different gate biases also causes distinct increments.

3.3.2 Gate Bias Effect on Unit-Lux Current

When we measure photo leakage current at fixed drain bias and different gate biases, as shown in Fig. 3-6(a), Unit-Lux Current increases with more negative gate bias slightly. Fig. 3-6(b) is the relationship between Unit-Lux Current versus gate bias under different drain biases.

Voltage difference between the drain and gate biases corresponds to the magnitude of electric field across the depletion region. So, a more negative gate bias means that the electric field would get stronger, as the same as a more positive drain bias does. Thus, from the result of our experiment, we can conclude that larger electric field across the drain depletion region should cause larger photo leakage current. Although both drain and gate bias affects the electric field strength in the depletion region, but they do in different ways. In the following section, we will discuss them in detail.

3.3.3 Analysis of Unit-Lux Current

We would like to know how much photo leakage current will be induced by the increasing biases. Consider a reasonable range that a LTPS TFT may operate while performing light sensing, the ratio of ULC at VD = 10 to ULC at VD = 2V is about 1.5~1.7, and ratio of ULC at VG = -10V to ULC at VG = -2V is about 0.95~1.2. The

variation from drain bias (ΔVD = 8V) causes larger Unit-Lux Current increment than gate bias (ΔVG = 8V).

On the other side, Fig. 3-5(b) tells us some other information about how drain and gate biases affect each other. Unit-Lux Current in the range about VD < 6V, gate bias effect is unapparent. In other words, gate bias causes almost no difference in photo leakage current when we apply drain biases that are not strong enough. When VD > 6V, gate bias effect would be significant and enlarges Unit-Lux Current when VG goes more negative. We can check this again according to Fig. 3-6(b), which shows when VD = 0.6V and 5.3V, Unit-Lux Current remains nearly unchanged when gate bias altered; when VD = 10V, gate bias increases Unit-Lux Current significantly when VG goes more negative.

From this phenomenon, we suppose that there're two different dominant mechanisms of Unit-Lux Current. When VD is small, ULC increases linearly with drain bias, and gate bias effect is trivial. When VD is large enough, ULC increases with drain bias more rapidly and gate bias effect becomes significant. We fit the ULC curve between VD = 0.6V ~ VD = 6V as shown by the dash line in Fig. 3-5(b), and assume the fitting curve is one of the two components of the total Unit-Lux Current, called ULC_{C1}. ULC_{C1} is the component that increase with drain bias linearly, and independent of gate bias. Following we subtract ULC_{C1} from the total ULC curve. This rest part of the total ULC is the second component called ULC_{C2}.

The dependence of ULC_{C2} on VD is shown in Fig. 3-7. It' s obvious to notice that ULC_{C2} increases with drain bias exponentially when VD is large enough, say, about VD > 8V. Therefore, Unit-Lux Current can be expressed by a linear combination of these two components:

$$\begin{aligned} \mathrm{ULC} &= ULC_{C1} + ULC_{C2} \\ &= (\alpha \mathrm{VD} + \beta) + \gamma \cdot \mathrm{e}^{(\mathrm{mVD\text{-}nVG})} \end{aligned} \tag{3.1}$$

$$\mathrm{ULC}_{C1} = (\alpha \mathrm{VD} + \beta) \tag{3.2}$$

$$\mathrm{ULC}_{C2} = \gamma \cdot e^{(\mathrm{mVD\text{-}nVG})} \tag{3.3}$$

The first term ULC_{C1} is proportional to VD and independent of VG. The second term is ULC_{C2} which increases with VD and VG exponentially. The values of fitting factors α, β, γ, m and n are listed in Table 3-2.

As shown in Fig. 3-8, this empirical formula agree with our experiment data very well, which supports our hypothesis that Unit-Lux Current is composed of two different leakage current components.

3.4 Temperature Effect on Unit-Lux Current

From the discussion above, we have separated the Unit-Lux Current into two different parts, ULC_{C1} and ULC_{C2}. Except the distinct dependence of drain biases, another significant difference between theses two components is that ULC_{C1} has almost no relationship with gate bias while ULC_{C2} does. We suppose that ULC_{C1} may be induced by mechanism like excess carrier diffusion or thermionic emission thus has weak dependence with electric field, especially gate bias. On the other hand, ULC_{C2} may be induced by mechanism like excess carrier drift or field emission thus has strong dependence on the drain and gate biases.

If these statements are correct, ULC_{C1} should be affect by temperature because it is induced by diffusion or thermionic emission. The influence of temperature effect on ULC_{C2} may be quite weak, because the dominant mechanism of ULC_{C2} is the electric field. In order to figure out the conduction mechanism of photo leakage current,

Unit-Lux Current at different temperatures has been measured. Table 3-3 shows the measure conditions.

We have to confirm that the correlation between Iphoto and illumination intensity at high temperatures is still linear first, thus the extraction of Unit-Lux Current could make sense. Fig. 3-9 shows the temperature effect on photo leakage current under a certain bias condition (VD, VG) = (10V, -5V). Photo leakage current was measured under 25, 40, 60, and 80 Celsius degree, and increases with higher temperature.

Drain bias dependence of Unit-Lux Current at different temperature is shown in Fig. 3-10. Unit-Lux Current in the range of VD = 0.6 ~ 6V has significant temperature effect, and higher drain bias reduces the temperature effect gradually. Therefore, ULC_{C1} is actually the term of temperature effect just as we expect.

We would like to discuss the relation between ULC_{C2} and temperature. After subtracting the fitting ULC_{C1} curves from total ULC curves, ULC_{C2} at different temperatures is shown in Fig. 3-11. Surprisingly, it demonstrates that ULC_{C2} is totally temperature independent which means ULC_{C2} is purely the term of photo leakage current induced by electric field.

Further analysis has been performed on ULC_{C1}. We have assumed that ULC_{C1} is the temperature dependent term, thus from equation 3.1 we know that factors α and β must be the functions of temperature. Fig. 3-12 shows the relationship between α and β and 1/kT. We find that these two factors increase with 1/kT exponentially and can be expressed as follow:

$$\alpha(T) = A \cdot e^{(-\frac{B}{kT})} \tag{3.4}$$

$$\beta(T) = C \cdot e^{(-\frac{D}{kT})} \tag{3.5}$$

A, B, C, and D are fitting factors, and the value of them are listed in Table 3-4.

We have divided Unit-Lux Current into two components. One of them would be affected by temperature, another is totally temperature independent. We suppose that ULC_{C1} is dominated by thermionic emission or carrier diffusion, ULC_{C2} is dominated by field emission or carrier drift. Although we have not enough evidence to prove the conduction mechanisms are correct or not, but the temperature experiments have at least agreed with our surmise.

3.5 Device Variation of Unit-Lux Current

The uniformity of poly-silicon thin film is always an important issue of LTPS TFTs. Different devices in the same process flow suffer from serious device variation and causes different characteristics. For this consideration we suspect that photo leakage current would also have variations between devices. Fig. 3-13 shows the photo leakage current of several devices on the same glass. It indicates that serious device variation of photo leakage current presents among our samples. Since all the fabrication flow and the TFT size is the same, and operation conditions like VD, VG, temperature is also identical, we suppose that the variation may comes from the different defect distribution or density in the grain boundary. Therefore, the effect of defect states on photo leakage current has been investigated in the later chapter.

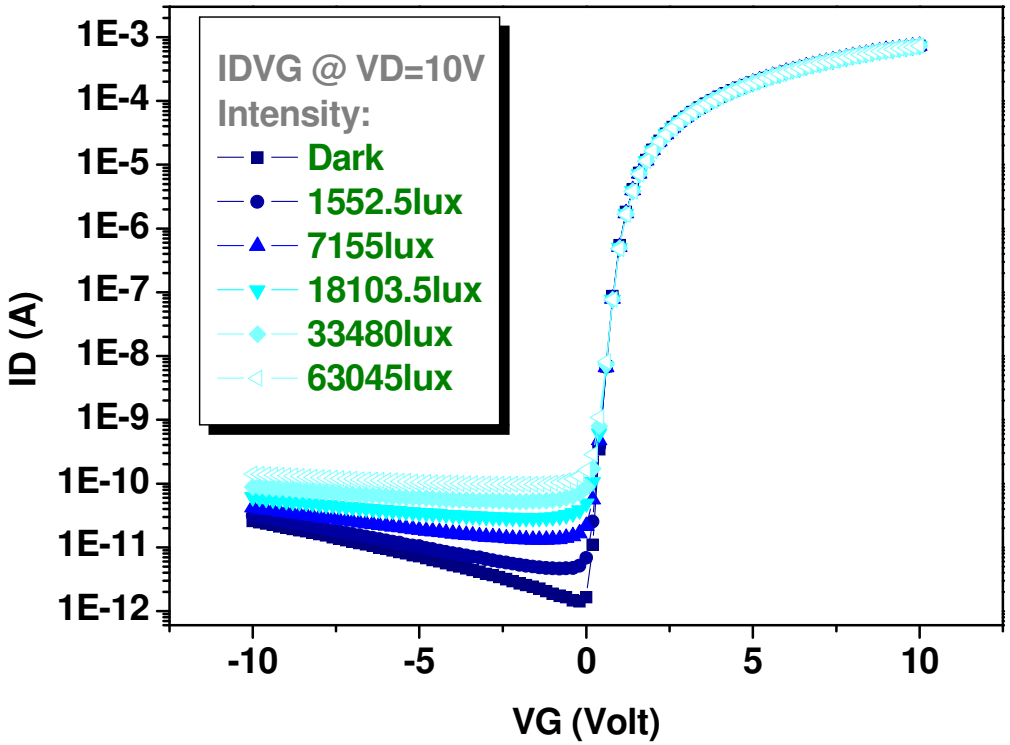

Fig. 3-1 (a) IDVG curve under illumination.

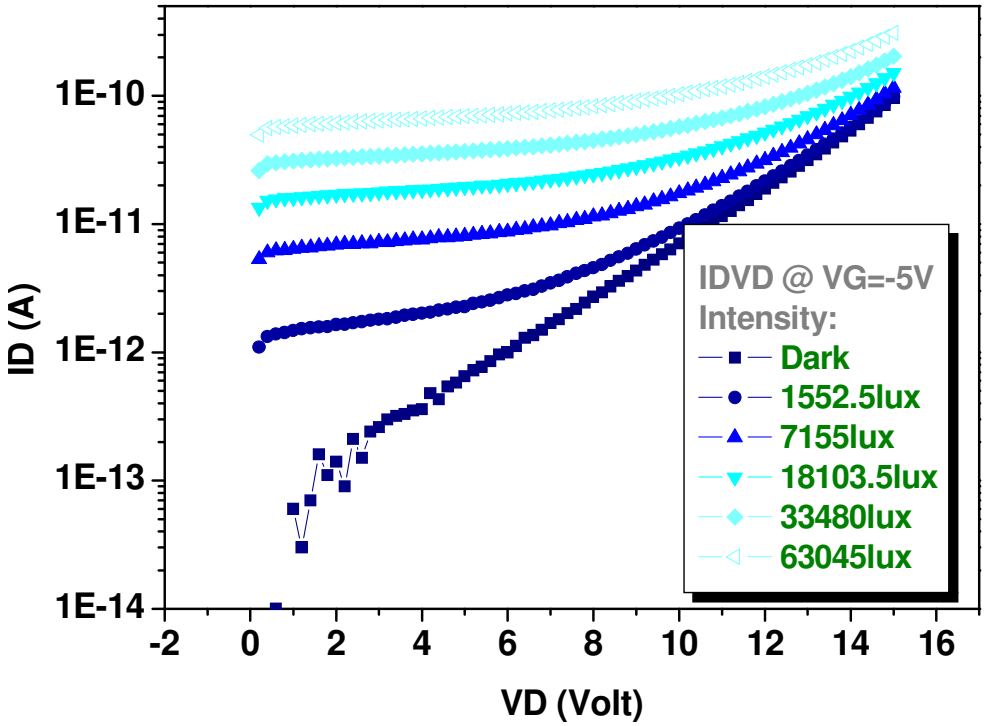

Fig. 3-1 (b) IDVD curve under illumination.

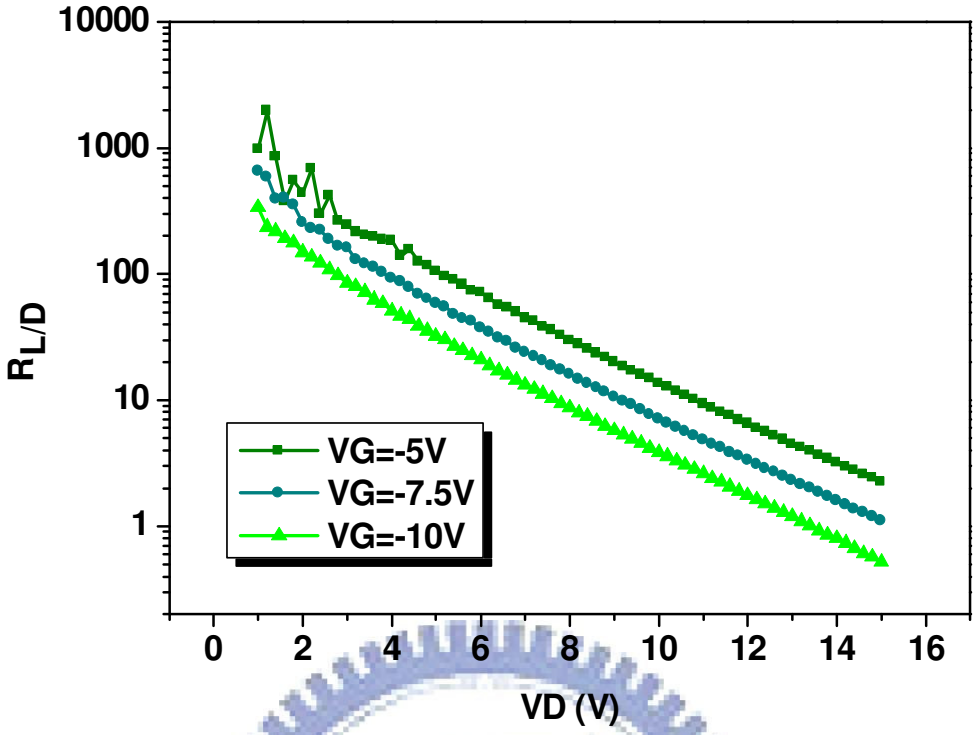

Fig. 3-2(a) Drain bias dependences of $R_{L/D}$.

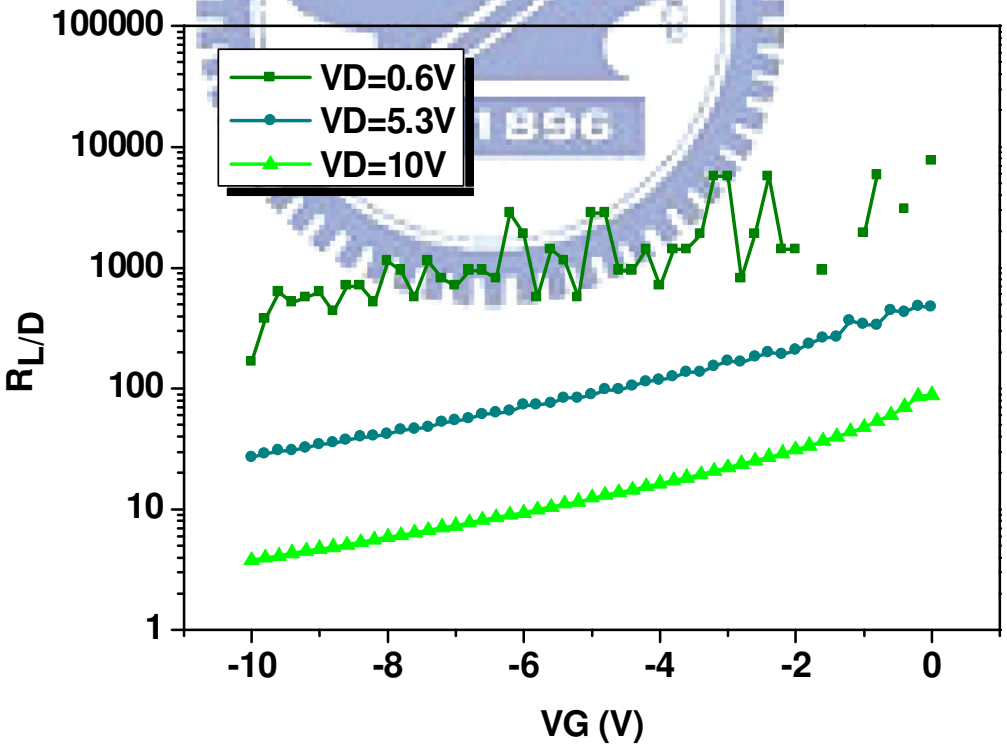

Fig. 3-2(b) Gate bias dependences of $R_{L/D}$.

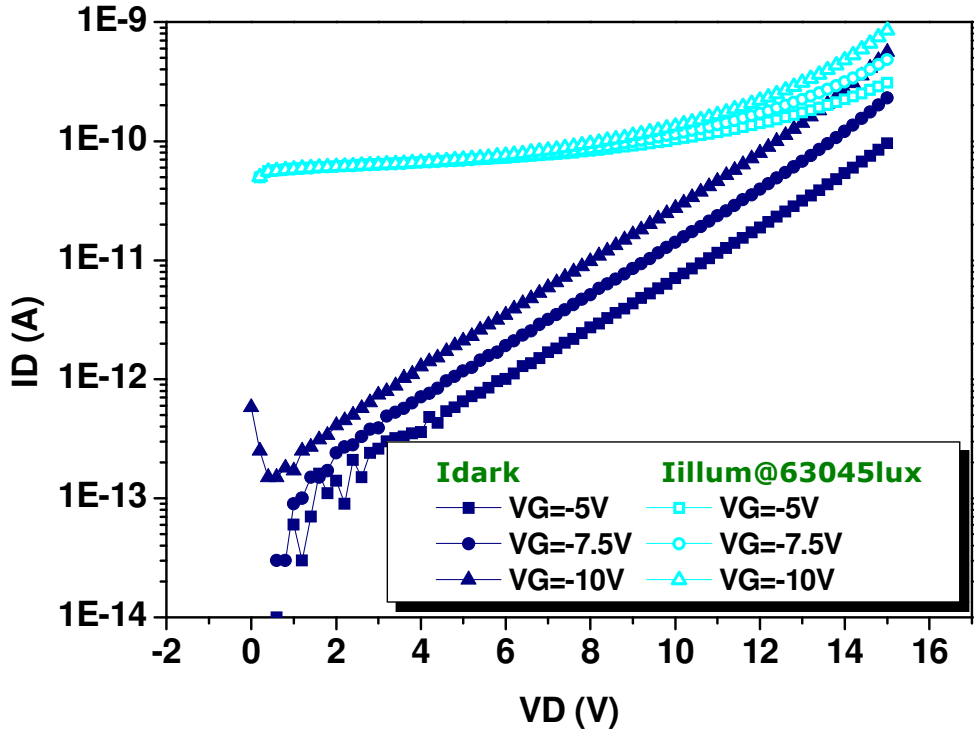

Fig 3-3 (a) Drain bias dependences of Iillum and Idark.

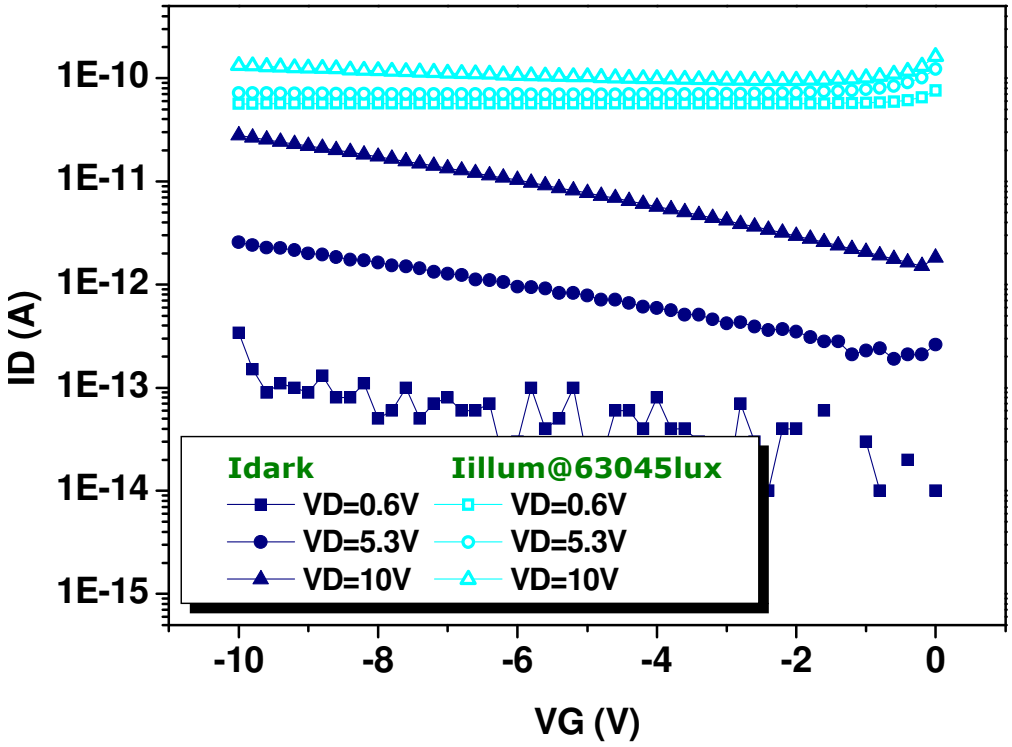

Fig. 3-3(b) Gate bias dependences of Iillum and Idark.

EXPERIMENT	Gate Bias (V)	Drain Bias (V)	Illumination Intensity (lux)
VG step VD sweep	-5	0.6 ~ 14 Interval: 0.2V	351
	-7.5		1553
	-10		7155
VD step VG sweep	-2~ -10 Interval:0.2V	0.6	18104
		5.3	33480
		10	63045

Table 3-1 Experiment conditions for VD, VG effects on photo leakage.

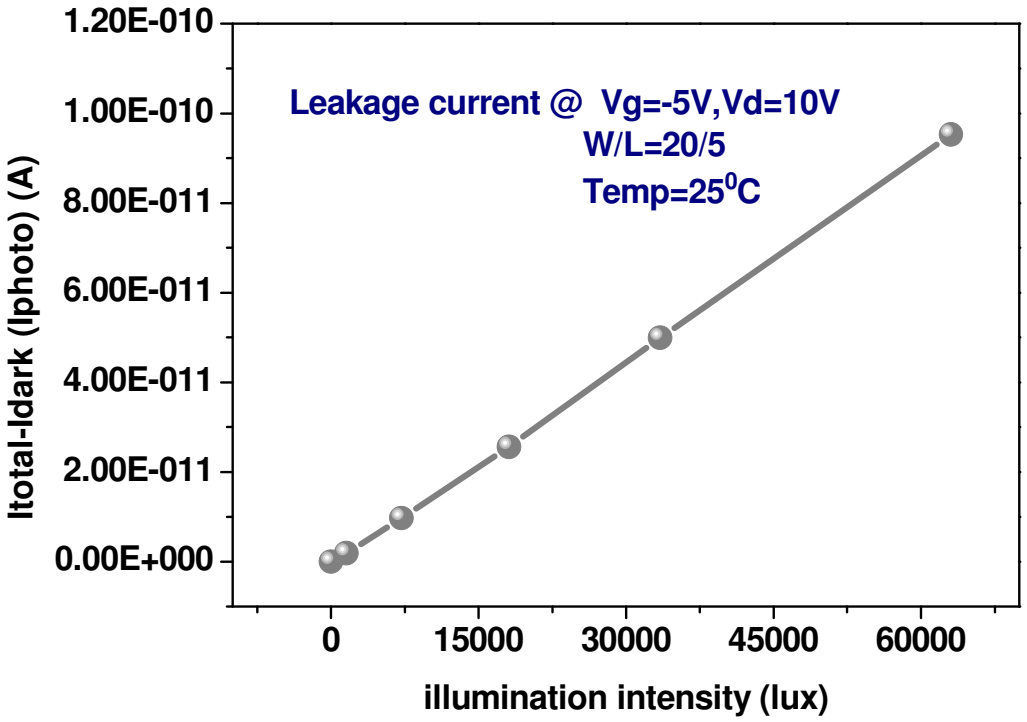

Fig. 3-4 Photo leakage current measured at different illumination intensity.

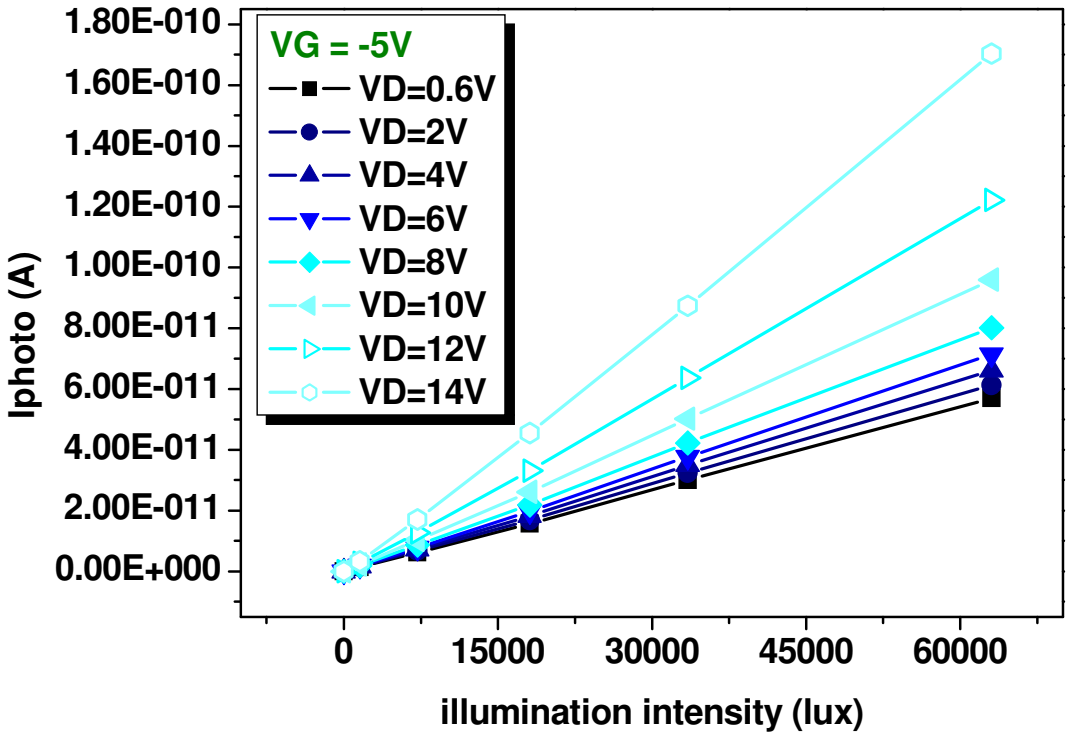

Fig. 3-5 (a) Photo leakage current at VG= -5V and VD=0.6V to 14V.

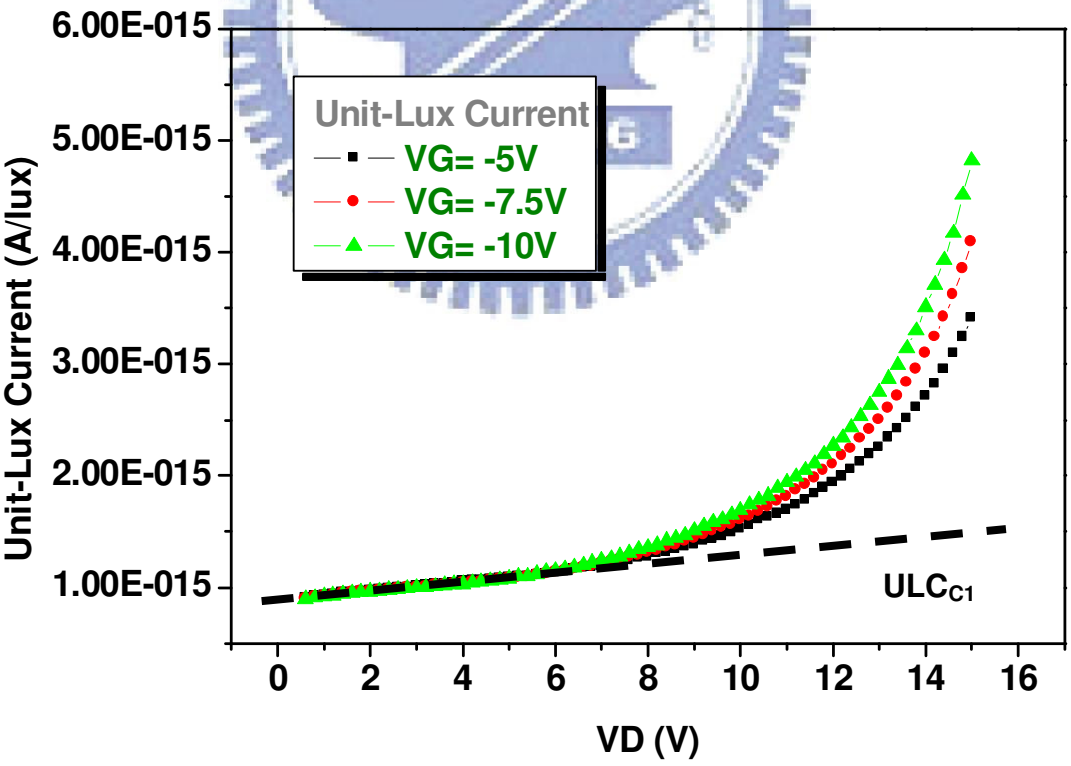

Fig. 3-5 (b) Drain bias effect on Unit-Lux Current at different gate biases.

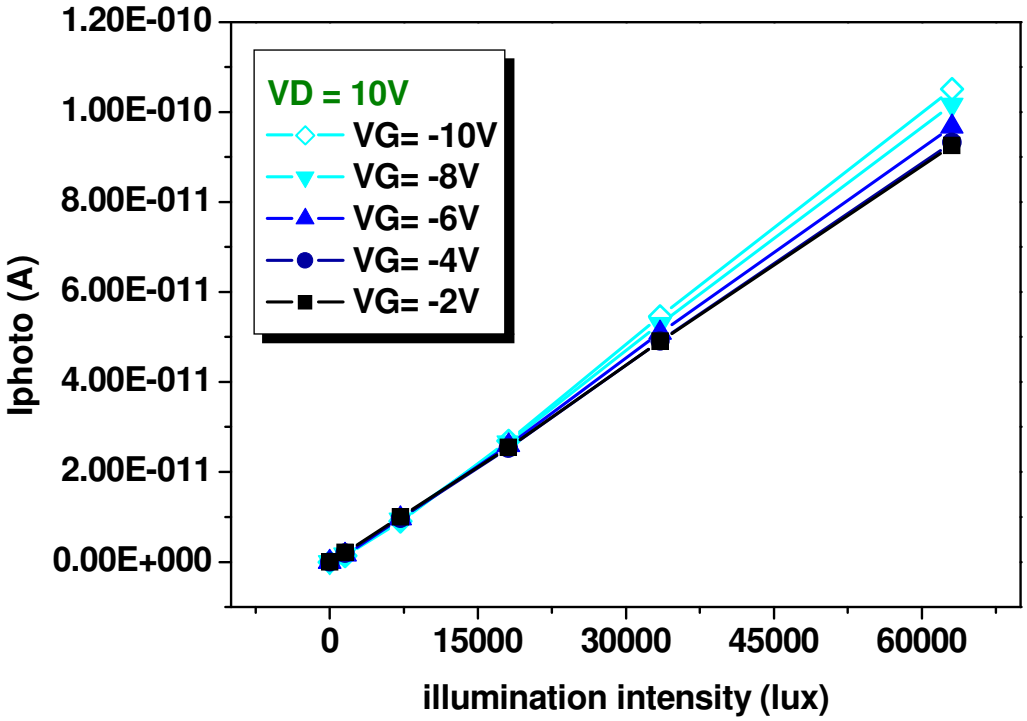

Fig. 3-6 (a) Photo leakage current at VD= 10V and VG= -2V to 10V.

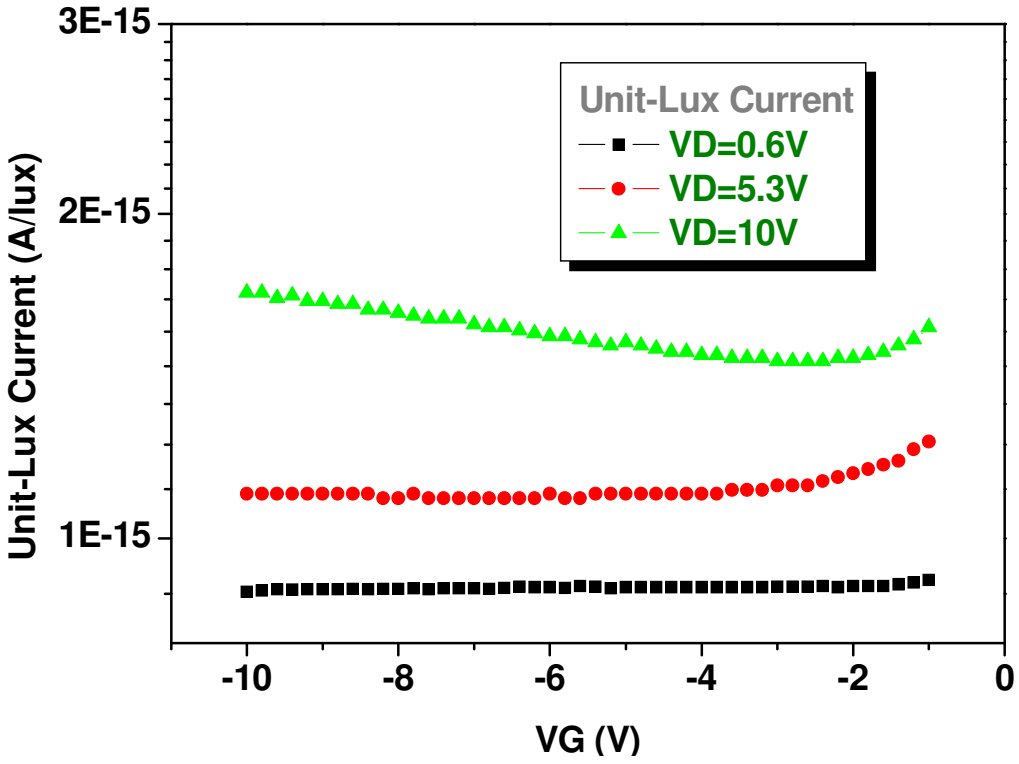

Fig. 3-6 (b) Gate bias effect on Unit-Lux Current at different drain biases.

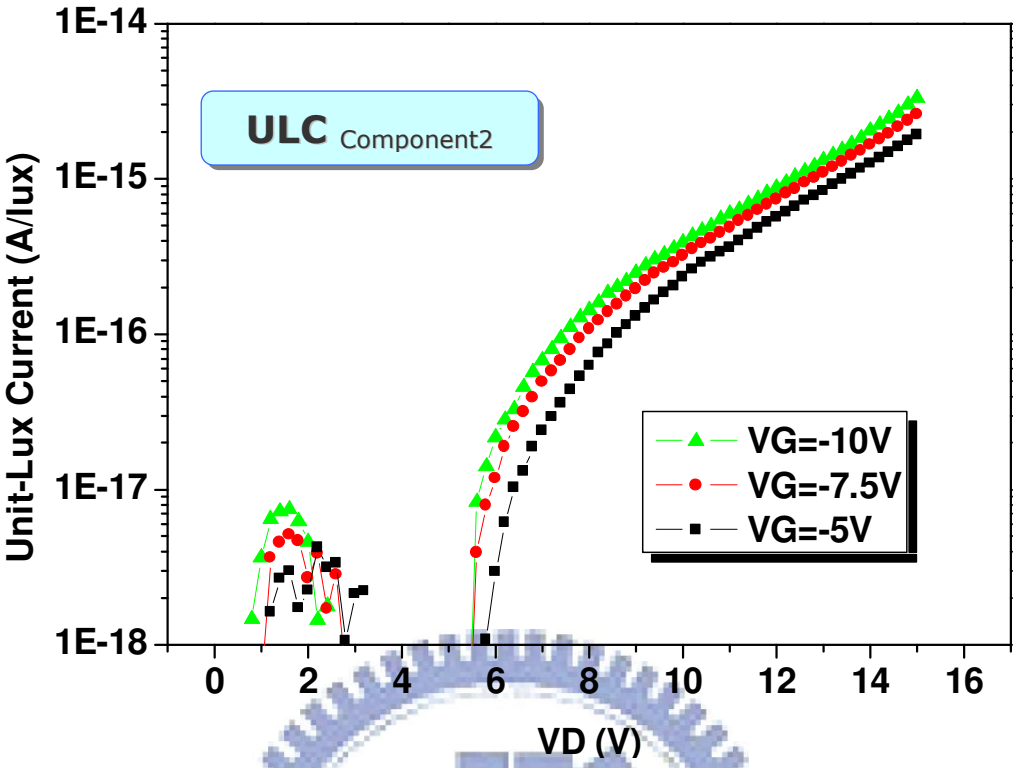

Fig. 3-7 The second component of Unit-Lux Current (ULC_{C2}) versus VD.

Fitting Factors	Value	Unit
α	$4X10^{-17}$	A/(V · Lux)
β	$8.8X10^{-16}$	A/(Lux)
γ	$1.61X10^{-18}$	A/(Lux)
m	0.42	1/V
n	0.135	1/V

Table 3-2 The values of fitting factors in equation (3.1).

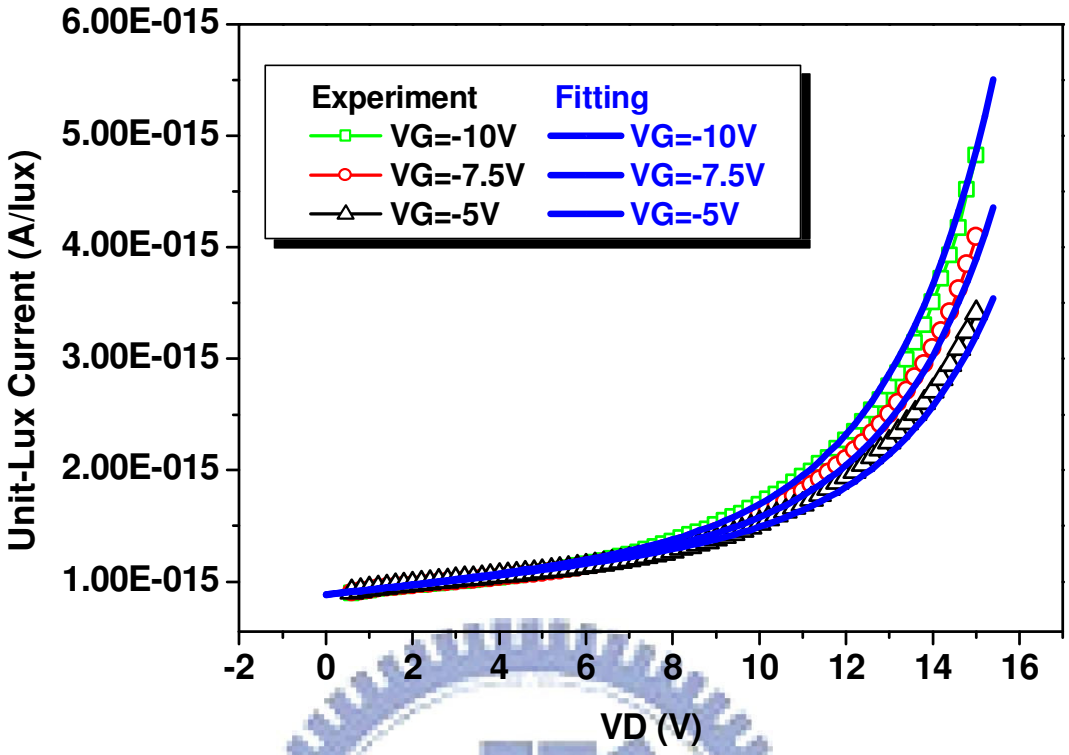

Fig. 3-8 Experiment data (symbols) and empirical formula (solid lines).

EXPERIMENT	Gate Bias (V)	Drain Bias (V)	Temperature (^{0}C)
VG step VD sweep	-5	0.6~15	25, 40, 60, 80
	-7.5		
	-10		

Table 3-3 Experiment conditions of temperature effect on photo leakage current.

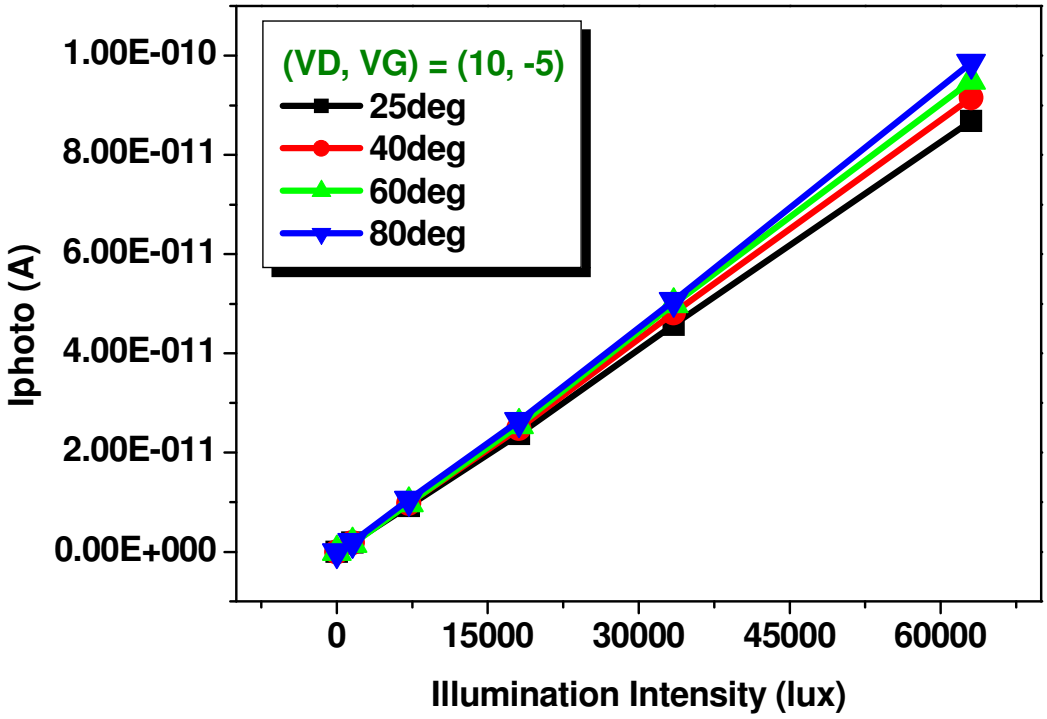

Fig. 3-9 Temperature effect on photo leakage current.

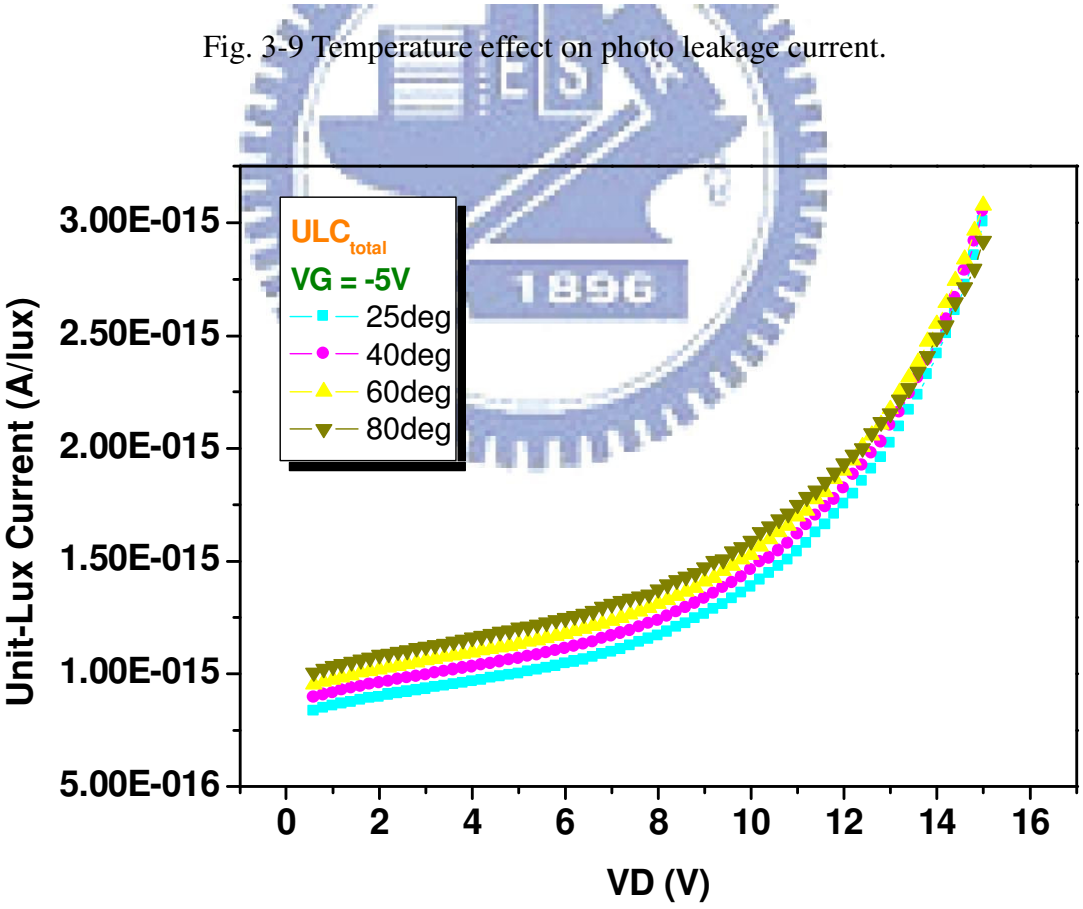

Fig. 3-10 Drain bias dependence of Unit-Lux Current at different temperature.

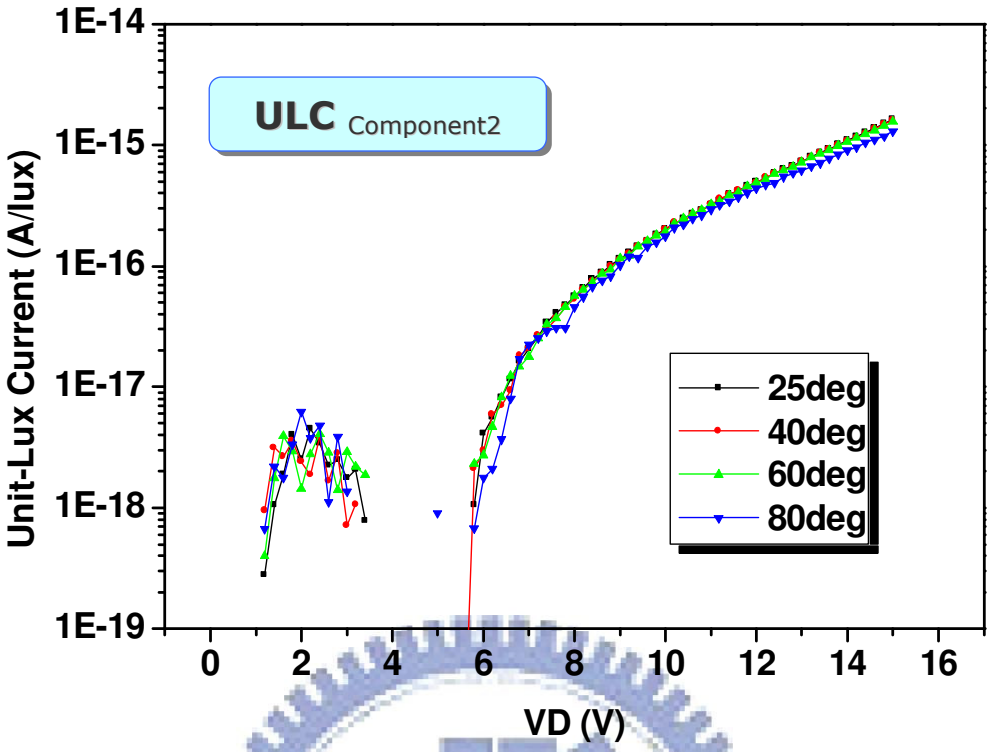

Fig. 3-11 ULC_{C2} at different temperature.

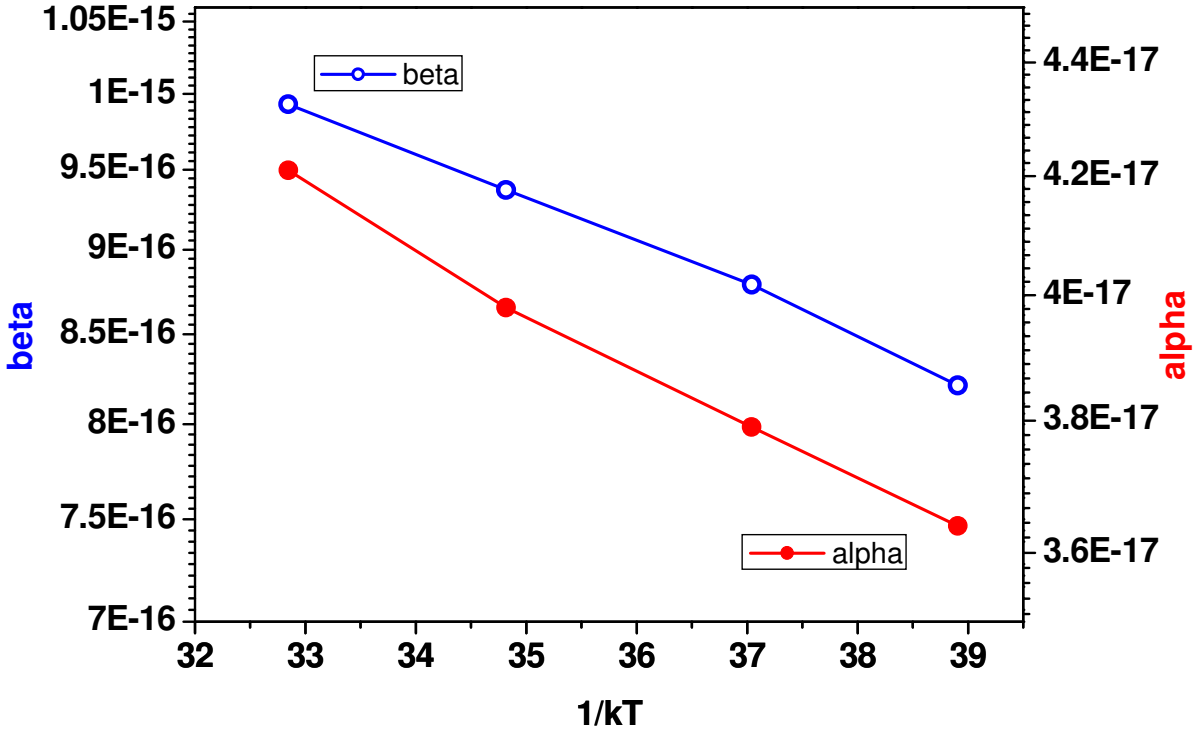

Fig. 3-12 Dependence of factors α and β on temperature.

Fitting Factors	Value	Unit
A	$9.16X10^{-17}$	A/(V · Lux)
B	0.02375	Joule
C	$2.76X10^{-15}$	A/(Lux)
D	0.03104	Joule

Table 3-4 The values of fitting factors in equation (3.4) and (3.5).

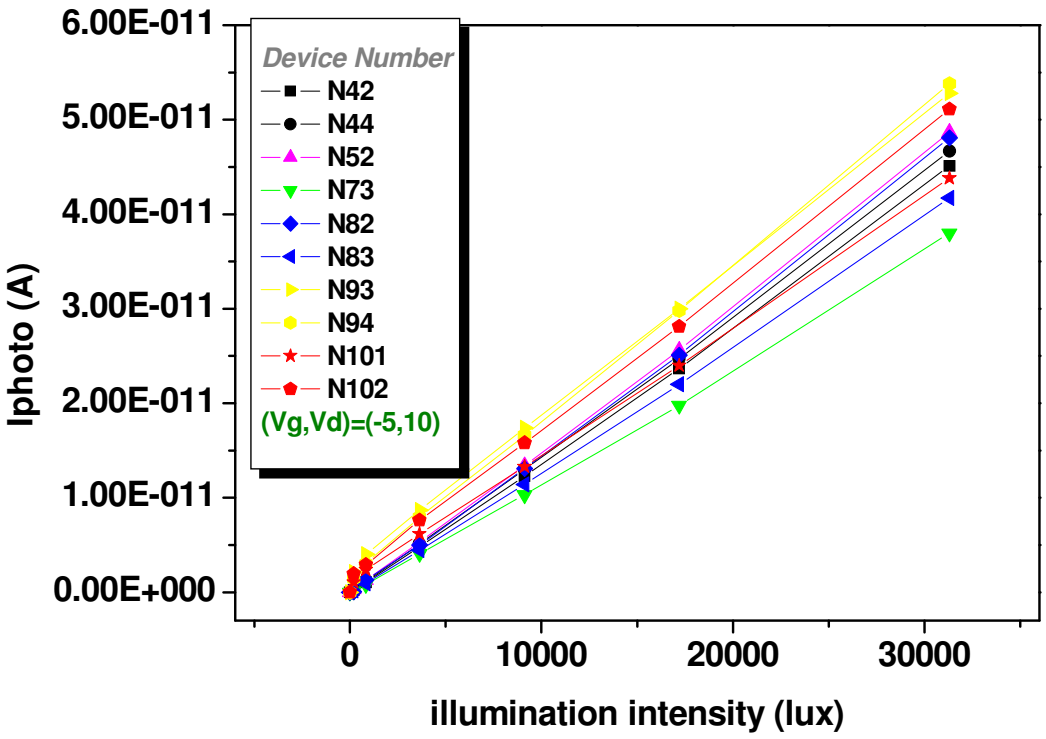

Fig. 3-13 Photo leakage current variation between different devices.

Chapter4

Photo Leakage Current after Extra Defect Creation

4.1 Extra Defect Creation by Hot Carrier Stress

4.1.1 Degradation Mechanism and Stress Condition

Degradation of the electrical characteristics due to hot carrier effect is an important issue in TFTs circuit application. Extensive investigation has shown that hot carrier induced defect states could be generated at the grain boundaries close to drain junction [6]. In our study, we utilize this electric degradation to create defect states and discuss the characteristics of photo-leakage current after these extra defects creation.

Fig. 4-1 shows the damage region after hot carrier stress. When a gate bias slightly greater than threshold voltage and a large drain bias applied on a TFT, high electric fields from the voltage difference between gate and drain will present in the junction depletion region. This field accelerates the electron-hole pairs to “hot carriers” with high kinetic energy and strike the lattice structure in this region. Avalanche multiplication due to impact ionization takes place at the drain end of the channel, thus leaves large amount of tail state strain bond defects here.

This degradation phenomenon causes severe decrease on the device mobility, as shown in Fig. 4-2. IV curve after stress altered significantly in both on and off region, the leakage current increase because of the defects act as a transient transfer center for carriers conducting, in the on region, however, these defects trap carriers would decrease the amount of carriers which are collected by drain electrode.

In our experiment, we stressed our devices at V_{GS} = 3V, and V_{DS} = 16V, and measured at different stress times of 1, 5, 25, 100, 500, 1000 sec. The later section will show how the photo leakage current altered after different level stress.

4.1.2 Photo Leakage Current Variation after Stress

Fig. 4-3 (a) shows photo leakage current measured at VG = -5V, VD = 10V after different stress times. We can find that the photo leakage current is lifted up after stress. The longer the stress time is, the higher Unit-Lux Current will be observed. Fig. 4-3 (b) is obtained from "reverse measurement". Reverse measurement is a method which applied the bias on the source electrode with grounded drain when measuring the leakage current (VG = -5V, VS =10V, VD = 0V). It means we can see the different leakage current behaviors with or without created defect states in the junction depletion region. Thus, from Fig. 4-3 (b) we noticed that if there's no extra defect states created in the junction depletion region, the photo leakage current remain almost unchanged after long time stress.

Fig. 4-4 shows the variation trend of Unit-Lux Current with different stress times. The plot shows the difference between forward and reverse measurement, which refers to the asymmetric defect distribution in the drain and source region separately. From the increasing Unit-Lux current we may reasonably suspect that: the created defect states enhance the photo leakage current.

4.1.3 Comparison between Unit-Lux Current Variation and Device Parameters

In previous sections we suppose the variation of Unit-Lux Current comes from the created defect states. The degradation due to stress should go along with the device parameter variation. Therefore, we would consider the parameter variation as evidence of defect states increasing.

The most useful parameters of LTPS TFTs are Mobility ($M\mu$), Threshold Voltage (Vth), and sub-threshold swing (SS). We can find out that after hot carrier stress, mobility is the most significant variation due to degradation, and the change in threshold voltage and sub-threshold swing is trivial. Fig. 4-5(a) demonstrated the variation trend of Vth and Unit-Lux Current with different stress time. Fig. 4-5(b) is the variation trend of SS and Unit-Lux current.

Good correspondence is gotten between mobility and Unit-Lux Current, as shown is Fig. 4-6 (a) and 4-6(b). The tendency of mobility and ULC is symmetric to each other. Fig. 4-6 (a) is mobility extracted from reverse measurement and Unit-Lux Current from forward measurement. Due to the channel pinch-off phenomenon, degradation behavior caused by drain region defects must relate to reverse mobility extraction; on the other hand, photo leakage current variation from drain region defects relates to forward Unit-Lux Current extraction. Similarly, Fig. 4-6 (b) is the correspondence of forward measured mobility and reverse measured Unit-Lux Current. This plot tells us that the undamaged source region almost doesn't lead to any variation of photo leakage current and device parameter.

4.1.4 ULC under Different VD, VG Conditions

In the last section 4.1.3, comparison between Unit-Lux Current and mobility variation of different level degradation is performed at VD = 10V, VG = -5V. We wonder if this trend would be the same under other off-region bias condition.

Fig. 4-7 (a) and Fig. 4-7 (b) demonstrate the gate and drain bias dependence of Unit-Lux Current after hot carrier stress. Distinct from the result of Fig. 3-3 (b) and 3-4 (b), the device after stress shows that gate bias effect become more insignificant than before. Fig.4-8 shows the variation tendency of Unit-Lux Current at (VD, VG) = (0.6V, -5 V), (0.6 V, -10 V), (10 V, -5 V), (10 V, -10 V). We can clearly see that

different gate biases causes nearly no difference on photo leakage current. From the results of Fig. 4-7 and 4-8, we may consider that the gate bias effect after hot carrier stress would become quite weak. Since that, after stress we will only focus on the variation tendency of Unit-Lux Current under different drain bias.

Fig. 4-9 is the comparison between Unit-Lux Current and mobility at VG = -5V, VD = 0.6V. Since we don't consider the gate bias effects after stress, what we've concerned about is that if the photo leakage current characteristics at VD = 0.6V cause the same result as the correspondence at VD = 10V. As we expect, decreasing device mobility with different stress periods refers to increasing Unit-Lux current. We may note that the mobility extracted from forward and reverse measurement is exactly the same, it's because the channel won't pinch-off at VD = 0.6V, thus forward and reverse mobility extraction can't distinguish the different defect distributions at source and drain region.

From these qualitative analyses above, we have confirmed that the behavior of extra created defect states would enhance the photo leakage current. We also find that at different bias conditions the variation trend of Unit-Lux Current is distinct, especially operation with different drain biases. Fig. 4-10 afford more precise comparison between Unit-Lux Current and mobility at VD = 10V and VD = 0.6V. The variation trends have been normalized, and then we can just pay attention on the increasing or decreasing tendencies of these different unit parameters. The result makes sense due to the good correspondence of ULC and M μ at VD = 10V and VD = 0.6V separately.

Therefore we've got concise conclusions in this section: Hot carrier stress creates a lot of tail state strain bond defects that enhance the photo leakage current, which the evidence of defect states creation is the decreasing on-current mobility.

4.2 Extra Defect Creation by Self Heating Stress

4.2.1 Degradation Mechanism and Stress Condition

LTPS TFTs, in most applications, are fabricated on glass substrates with poor thermal conductivity. Therefore, as the applied V_{GS} and V_{DS} are high, the heat resulting from the high current flow and voltage difference in the channel may be difficult to dissipate. The accumulated heat causes the Si–H bonds to break, which in turn increases the deep states dangling bond in the channel. This degradation is known as Self Heating effect [7].

Although this thermal degradation phenomenon may induce a lot of defect state in the whole poly-si thin film, in this thesis, however, we use a simplified model of defect distribution in the thin film as shown in Fig. 4-11 to discuss the photo effect.

The states created by self heating stress apparently affect the transfer characteristic of the device mainly in on- and sub-threshold region. Fig. 4-12 is the IV curve of our sample after self heating stress. Except the lower mobility, serious threshold voltage shift is the most important feature of self heating stress. The physical meaning is that there are numerous deep states in the mid gap to be filled before the device is turned-on.

In our experiment, we stressed our device at V_{GS} = 15V, and V_{DS} = 15V, and measured at different stress times of 1, 5, 25, 100, 500, 1000 sec. The later section will show how the photo leakage current altered after different levels of stress.

4.2.2 Photo Leakage Current Variation after Stress

Fig. 4-13 (a) shows photo leakage current measured at V_G = -5V, V_D = 10V after different stress times. Different from hot carrier stress, we can find that the photo leakage current falls after self heating stress. The longer the stress time is, the lower Unit-Lux Current is observed. Fig. 4-13 (b) is obtained from reverse measurement.

From these two plots we will get some information about the location of created defect states in the channel.

Variation trends of Unit-Lux Current with different stress time are demonstrated in Fig.4-14. Very dissimilar trends are observed from forward and reverse measurement, which indicates that the amount of defect states may not be the same in source and drain regions. Even more, reverse measurement curve varies in an unusual way. Unit-Lux Current measured by reverse bias condition is lifted up in the early five seconds, and decreases after longer stress time as well as forward measurement. We will discuss this special phenomenon later.

However, different from hot carrier stress, the decreasing Unit-Lux Current after self heating stress suggests that the created defect states suppress the photo leakage current.

4.2.3 Comparison between Unit-Lux Current Variation and Device Parameters

Similar to section 4.1.3, we perform comparison between ULC and device parameters after Self Heating stress. After stress, significant degradation on M μ and SS is observed. But poor correspondence between these two device parameters and Unit-Lux Current occurs, as shown in Fig. 4-15 (a) and 4-15 (b).

On the other hand, good correspondence is gotten between threshold voltage and Unit-Lux Current, as shown in Fig. 4-16 (a) and 4-16(b). The tendency of Vth and ULC is symmetric to each other. As we mentioned in previous section, due to the channel pinch-off phenomenon, degradation behavior caused by drain region defects must relate to reverse Vth extraction. Furthermore, photo leakage current variation from drain region defects relates to forward Unit-Lux Current extraction. Similarly, forward Vth and reverse Unit-Lux Current extraction was compared for observation

of source region defect states effect.

4.2.4 ULC under Different VD, VG Conditions

Comparison between Unit-Lux Current and device parameters has been performed at VD = 10V, VG = -5V. Thus, gate and drain bias dependences of Unit-Lux Current after Self Heating stress would be discussed in this section. Fig. 4-17 (a) and Fig. 4-17 (b) demonstrate the gate and drain bias dependence of Unit-Lux Current after Self Heating stress. Fortuitously, gate bias effect has been reduced after Self Heating stress as the case of Hot Carrier stress.

In Fig. 4-18, variation tendency of Unit-Lux Current at (VD, VG) = (0.6V, -5 V), (0.6 V, -10 V), (10 V, -5 V), (10 V, -10 V) were compared. It indicates that after stress, different gate bias causes less difference in the variation trend of ULC than drain bias. Therefore, we will only focus on the variation tendency of Unit-Lux Current under different drain bias, and consider gate bias as minor effect in ULC after stress.

Fig. 4-19 is the comparison between Unit-Lux Current and mobility at VG = -5V, VD = 0.6V. Increasing threshold voltage with different stress periods refers to decreasing Unit-Lux Current, just the similar trend as we've got at VG = -5V, VD = 10V. We also note that the Vth extracted from forward and reverse measurement is almost the same, it's because the channel pinch-off phenomenon won't occur at VD = 0.6V, thus forward and reverse mobility extraction can't distinguish the different defect distributions at source and drain regions.

Normalized Vth and ULC at VD = 10V and 0.6V are compared in Fig. 4-20. We would like to analyze these factors more precisely. Contrast to the curves at VD = 10V, we find that at VD = 0.6V the correspondence between ULC and Vth seems that they do not exhibit the same trend. We attribute this result to the different depletion widths induced by different drain bias. Self Heating stress creates a lot of defect states in the

whole poly-Si thin film and because of the depletion region width at VD = 0.6V is smaller than VD =10V, defect states included in a narrow depletion region must less than a wide depletion region. Therefore, Unit-Lux Current reducing due to these defect states at VD = 0.6V couldn't reflect the total effect of these created defect states, while VD = 10V could do better. Thus, better correspondence between ULC and Vth is gotten at VD = 10V, while the case of VD = 0.6V is not perfect.

However, even the correspondence between ULC and Vth is not exactly well at VD = 0.6V, the qualitative discussions still suggest our conclusion in this section: Self heating stress creates a lot of deep state dangling bond defects that reduces the photo leakage current, the evidence of defect states creation is the increasing device threshold voltage.

4.3 Discussion of Carrier Recombination Process

We have summed up two interesting conclusions in previous sections. Different defect states in the energy gap cause entirely different results on photo leakage current, Tail state strain bonds enhance photo leakage current, while deep state dangling bonds reduce it. We discuss this phenomenon by the recombination mechanism of excess carrier injection.

Fig. 4-21 shows the scheme of the recombination process. Electron-hole pairs in the indirect semiconductor like silicon must recombine with each other through a trap center located in the energy gap. When a pair of electron and hole is injected to the conduction and valance bands, the recombination process contains two steps: Firstly, the hole would be trap in a defect state when going through the energy gap, where this step is called "hole capture". Following immediately is "electron capture" which means the electron is trapped by the same defect state and annihilate with the hole.

Due to some reasons like thermal vibration of the lattice structure, electron capture process does not always happen after hole capture. The hole trapped by the defect state may be emitted back to valance band, consequently the recombination process is delayed. This special case is called “thermal re-excited”.

Therefore, tail states created by hot carrier stress may enhance the photo leakage current because these defects located close to either conduction band or valance band. They have strong probability for carriers to be thermal re-excited and then delay the recombination. Since recombination would be delayed easier, the photo leakage current increasing is an inevitable consequence.

On the other hand, deep state defects created by self heating stress reduce the photo leakage current, because the mid-gap location would have less probability for thermal re-excited phenomenon. So, recombination may be enhanced after these mid-gap defect states creation, and result in the decrease of photo-leakage current.

The unusual characteristic in the reverse measurement of Unit-Lux Current after self heating stress (Fig. 4-14) could be explained now. In the early five seconds, the stress time is not long enough for the accumulated heat to break the Si-H bonds, and the voltage difference between gate and source (VGS) may induce a lot of unbroken strained bonds near the source region and then increase the photo leakage current slightly. As stress time increasing, Si-H bonds would be broken by heat and left numerous deep state dangling bonds that suppress the photo leakage current, as well as the result of forward measurement.

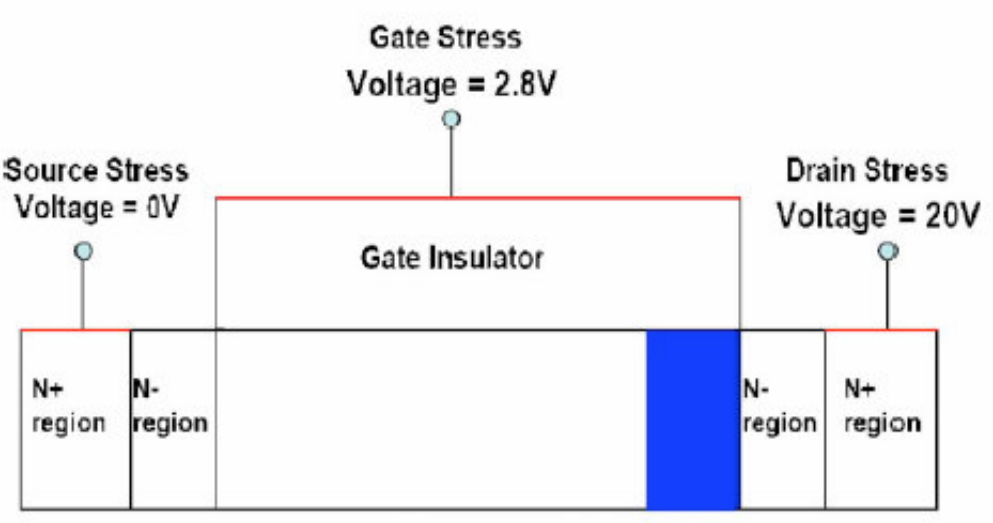

Fig. 4-1 Scheme of damage region in a LTPS TFT after Hot Carrier Stress.

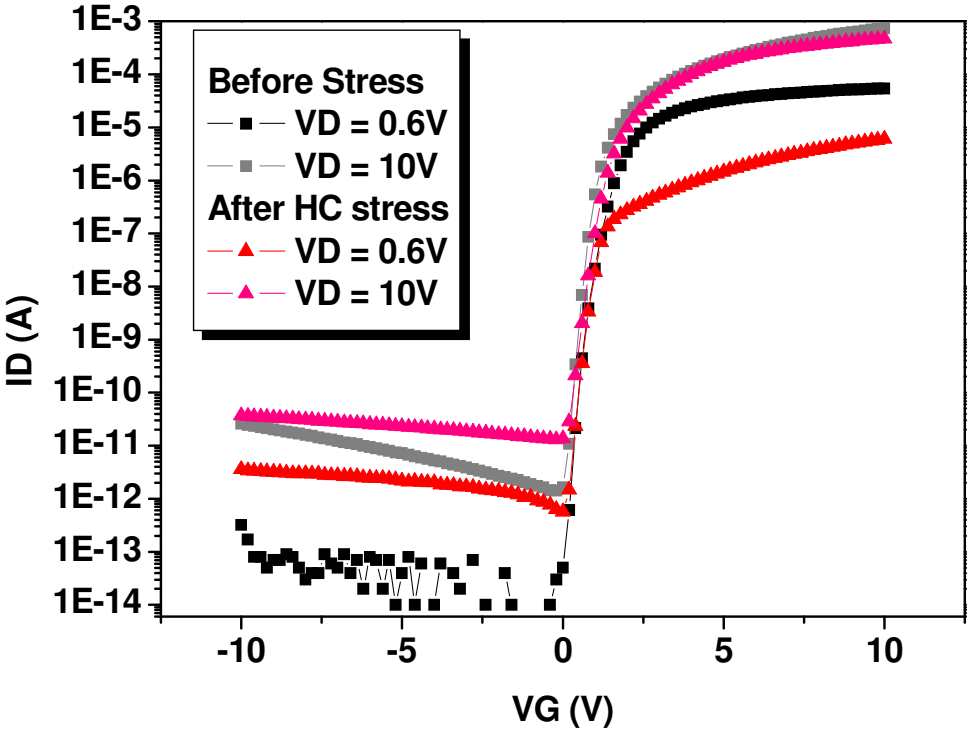

Fig. 4-2 IV curves before and after Hot Carrier stress.

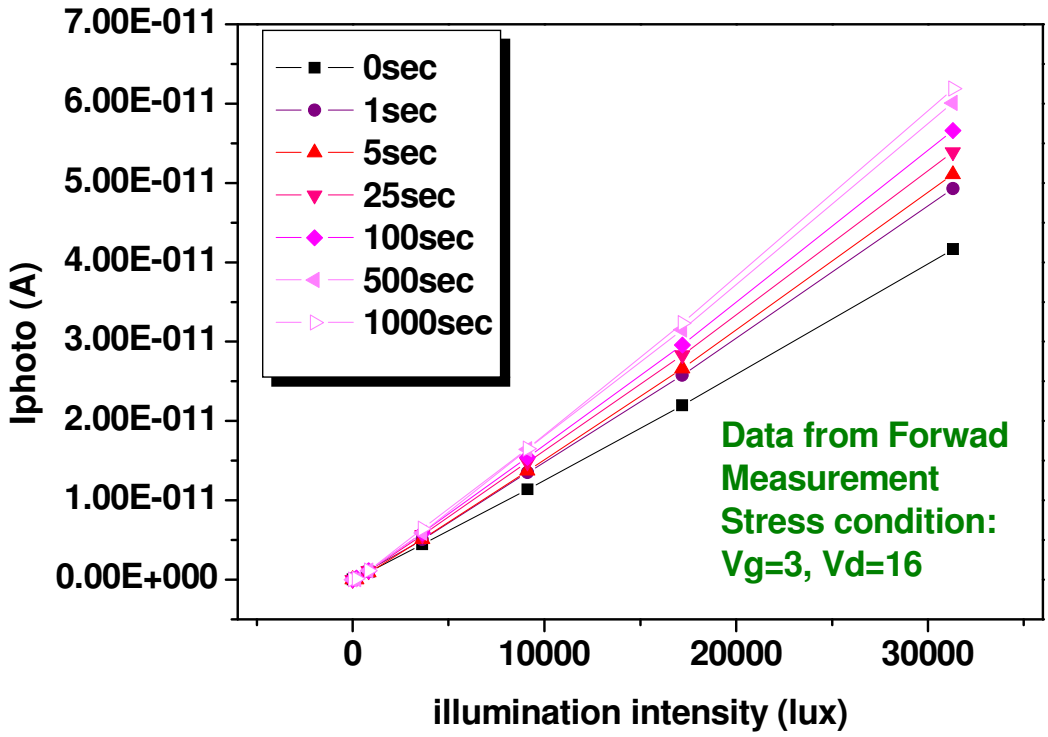

Fig. 4-3 (a) Photo current after Hot Carrier stress with different stress time (Forward).

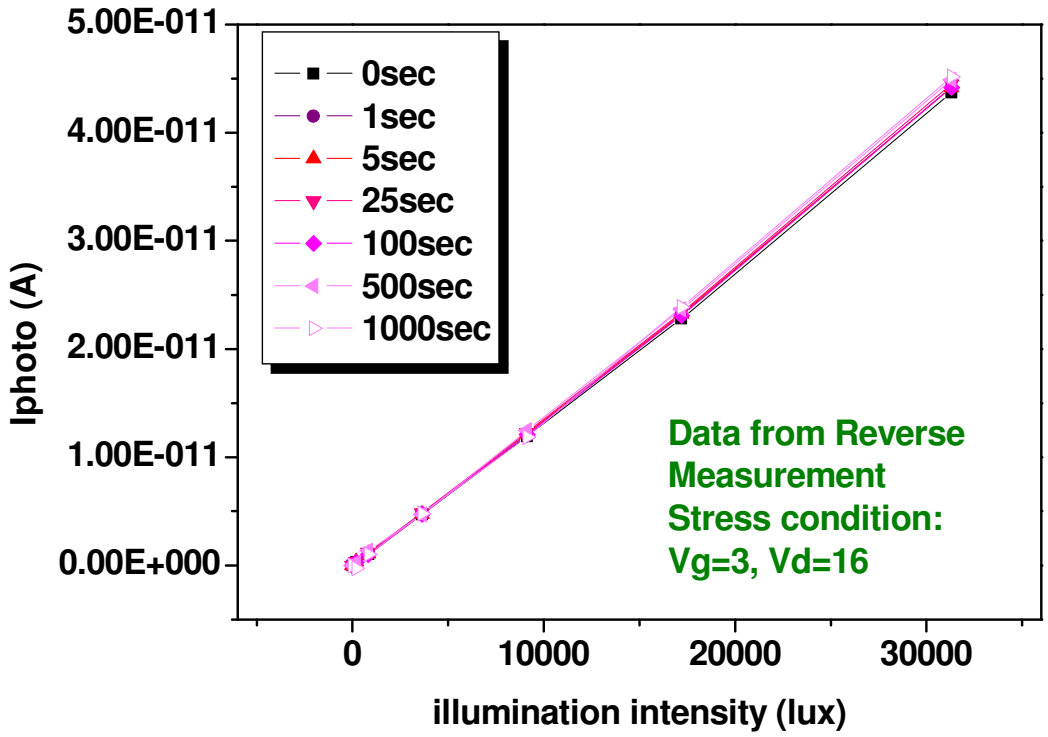

Fig. 4-3 (b) Photo current after Hot Carrier stress with different stress time (Reverse).

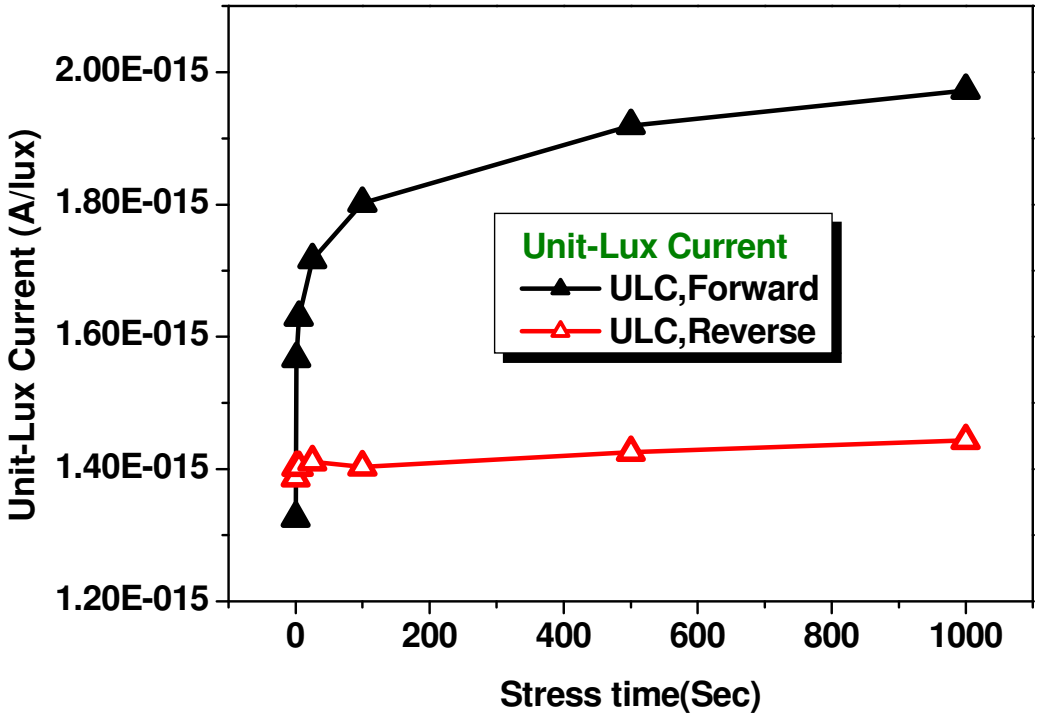

Fig. 4-4 Unit-Lux Current at (VD, VG) = (10V, -5V) with different stress time.

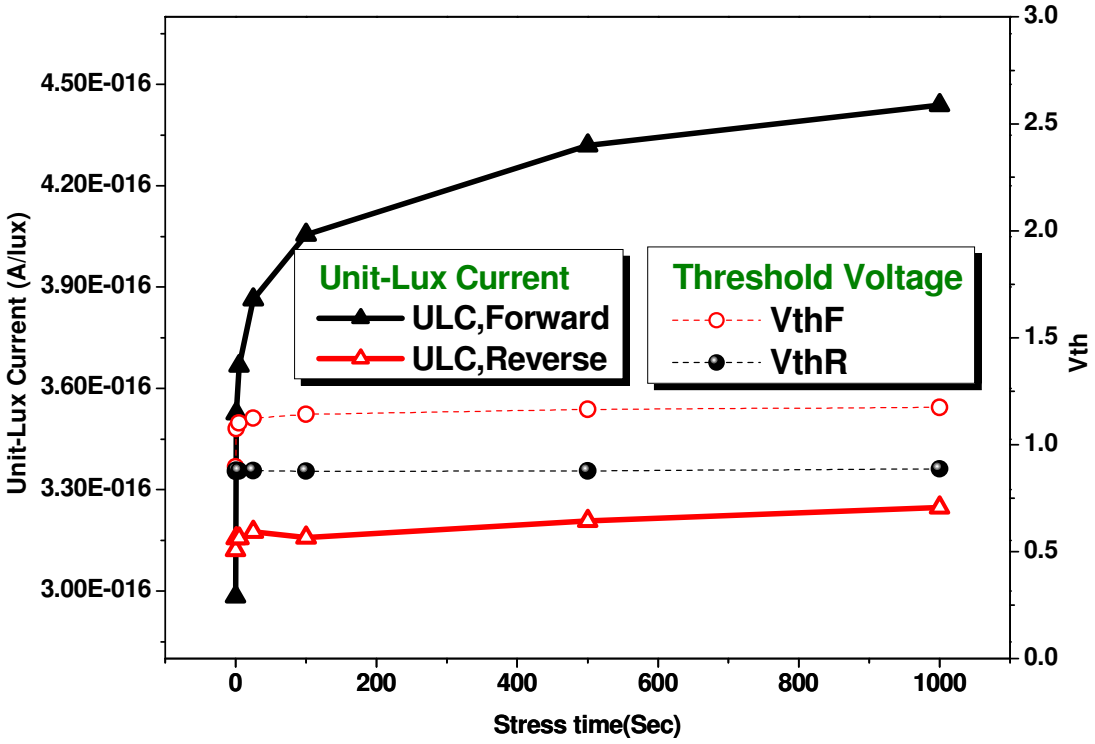

Fig. 4-5 (a) Variation trends of Vth and Unit-Lux Current with different stress time.

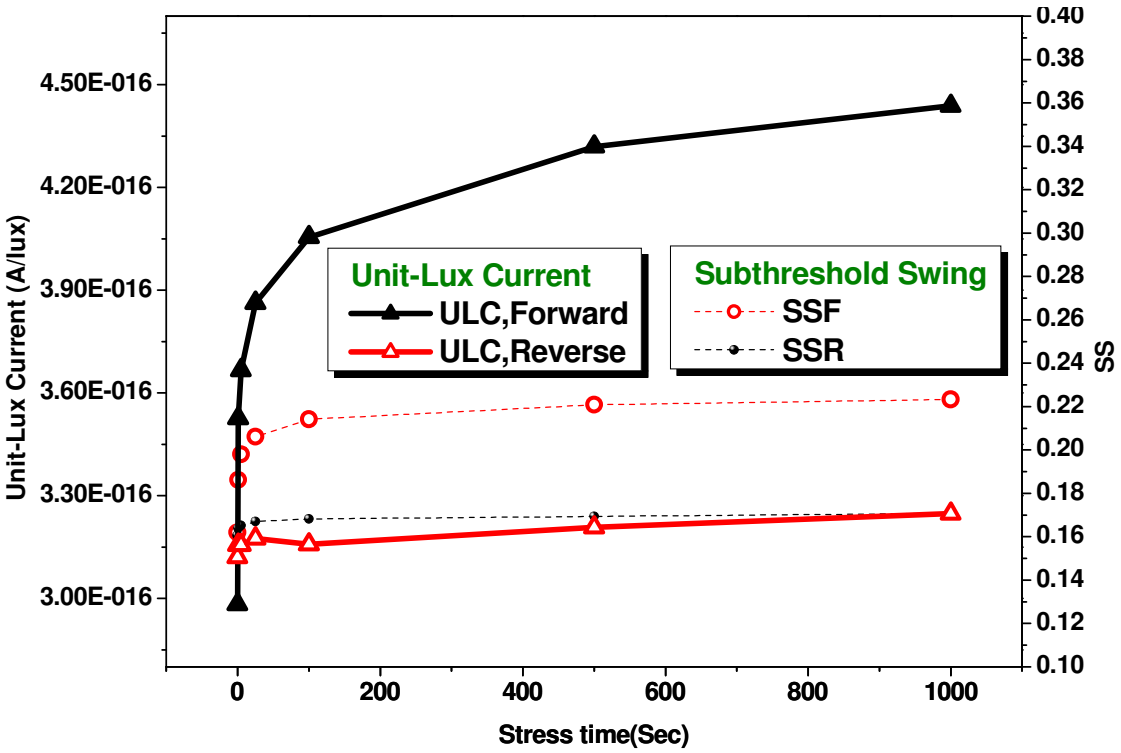

Fig. 4-5 (b) Variation trends of SS and Unit-Lux Current with different stress time.

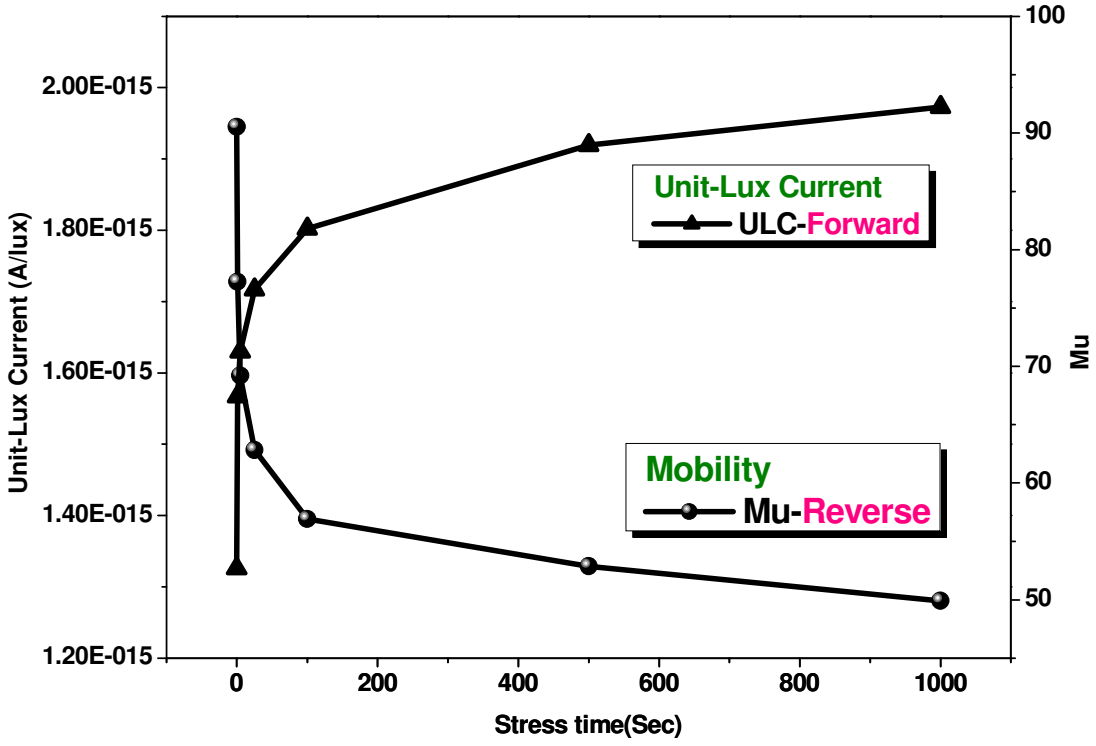

Fig. 4-6 (a) Reverse measured mobility and forward measured Unit-Lux Current.

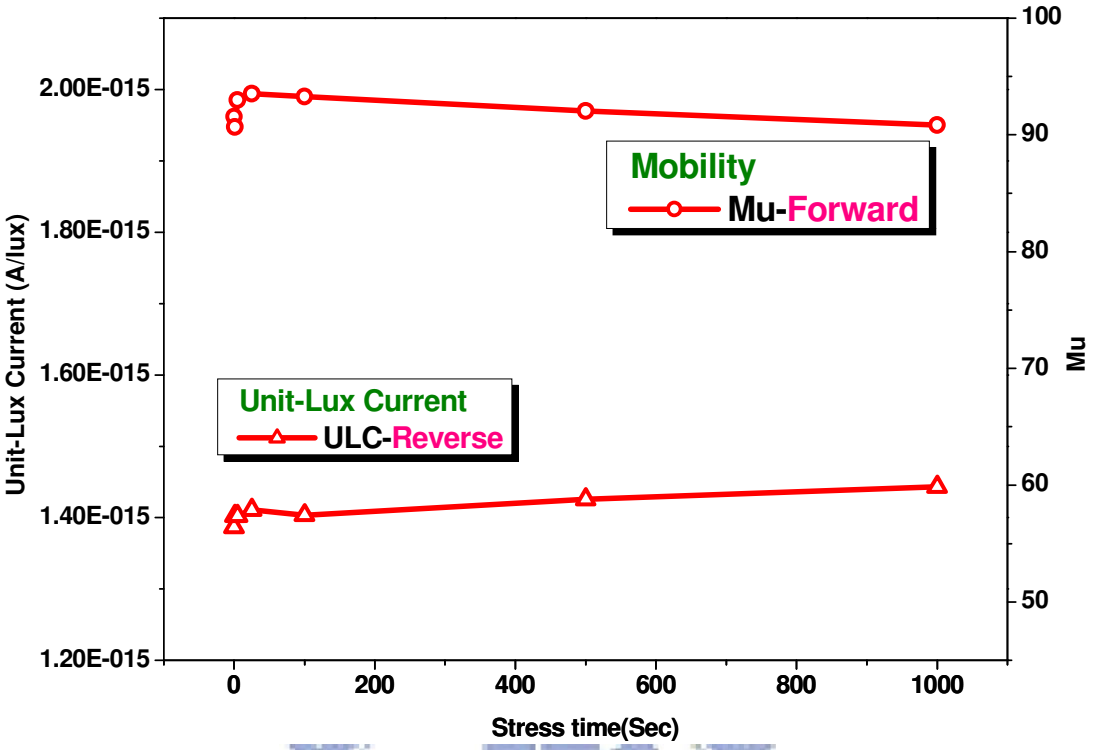

Fig. 4-6 (b) Forward measured mobility and reverse measured Unit-Lux Current.

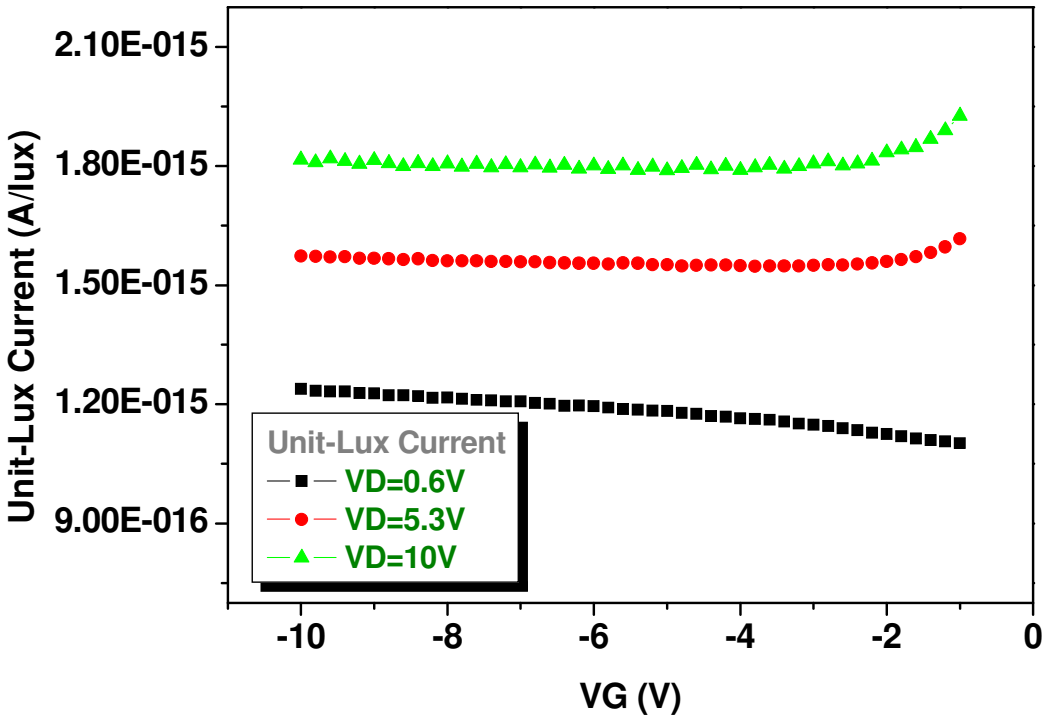

Fig. 4-7 (a) Gate bias dependence of Unit-Lux Current after Hot Carrier stress.

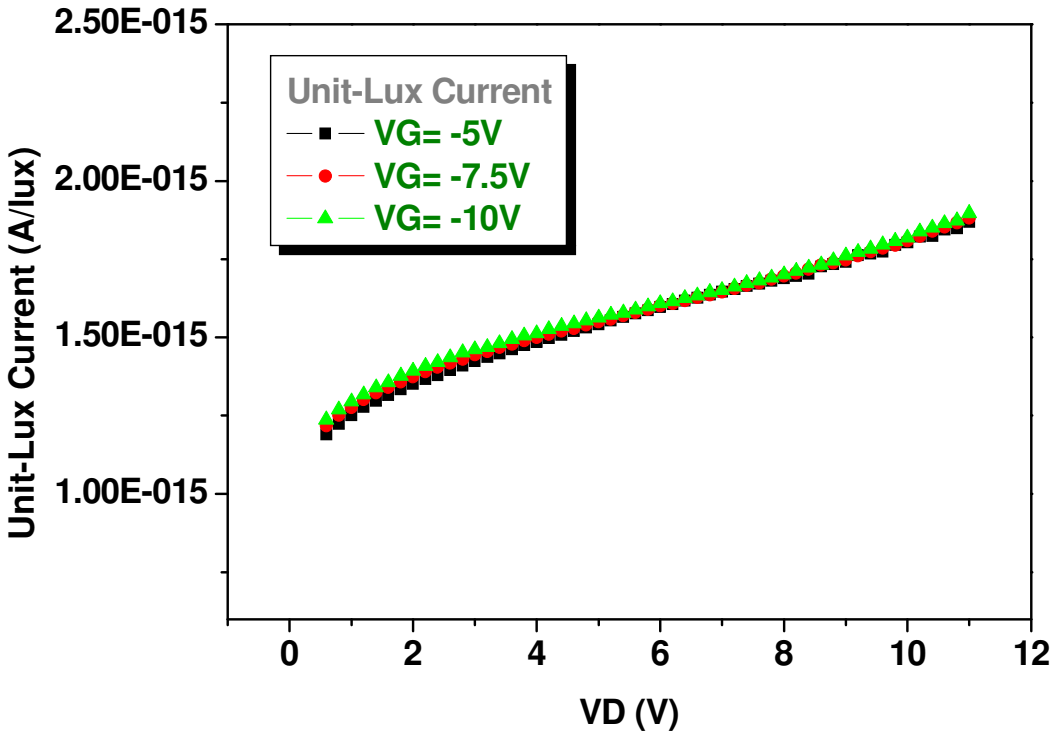

Fig. 4-7 (b) Drain bias dependence of Unit-Lux Current after Hot Carrier stress.

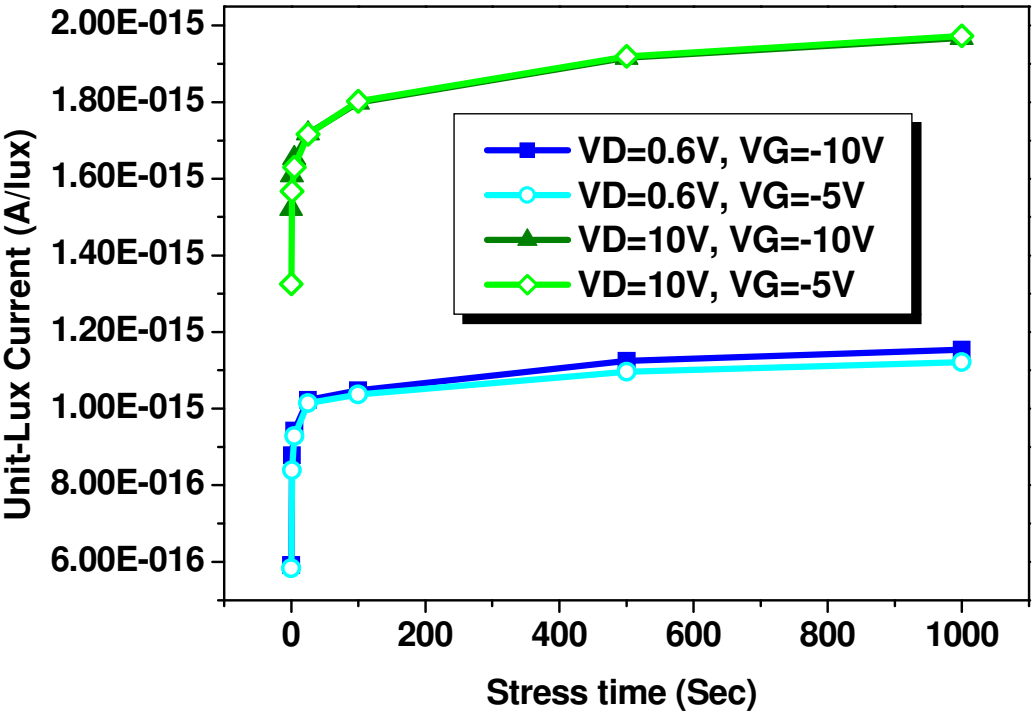

Fig. 4-8 Variation trends of Unit-Lux Current at different bias conditions.

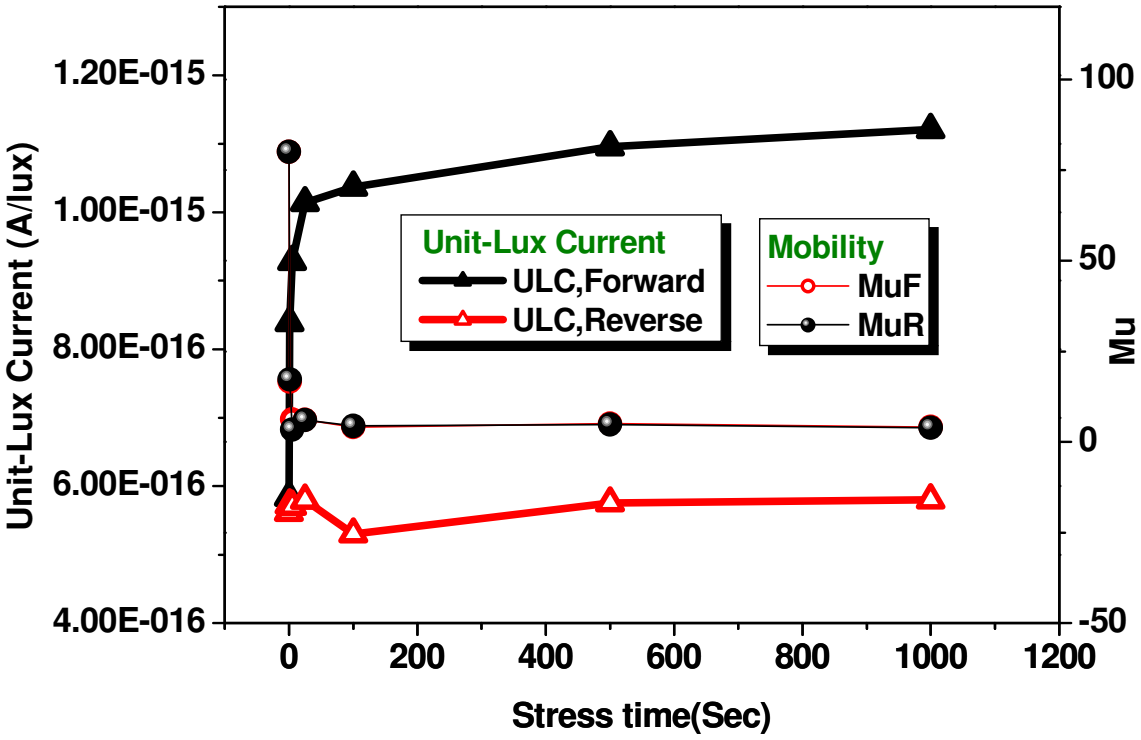

Fig. 4-9 Variation trends of M μ and Unit-Lux Current at VD = 0.6V.

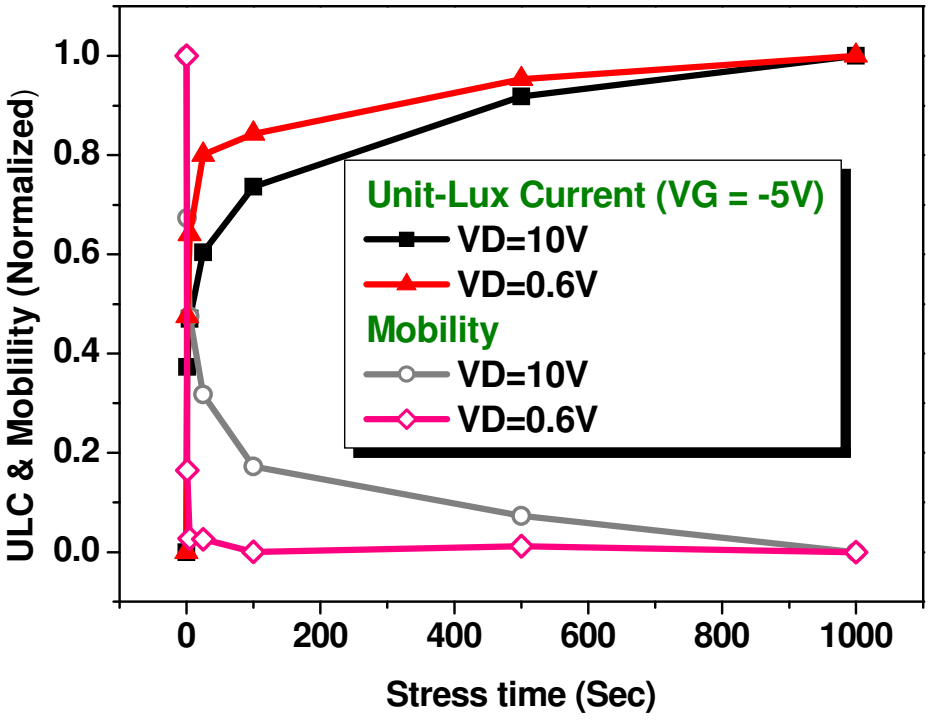

Fig. 4-10 Normalized Unit-Lux Current and mobility at VD = 10V and VD = 0.6V.

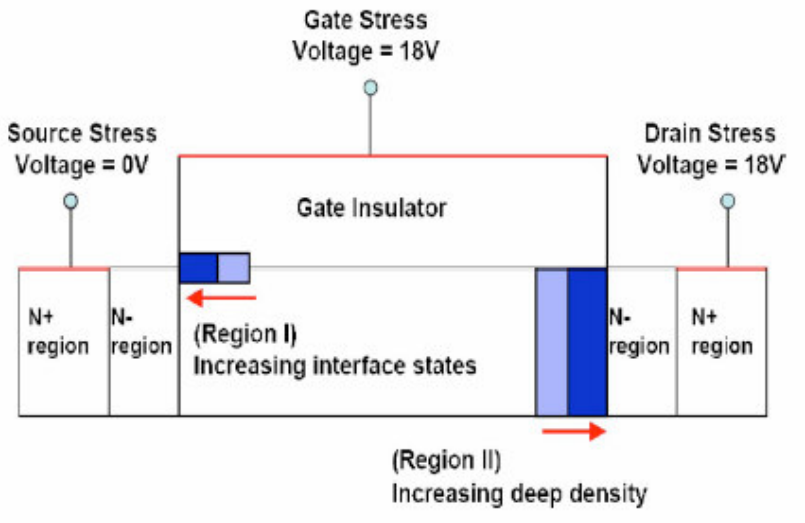

Fig. 4-11 Scheme of damage region in a LTPS TFT after Self Heating Stress.

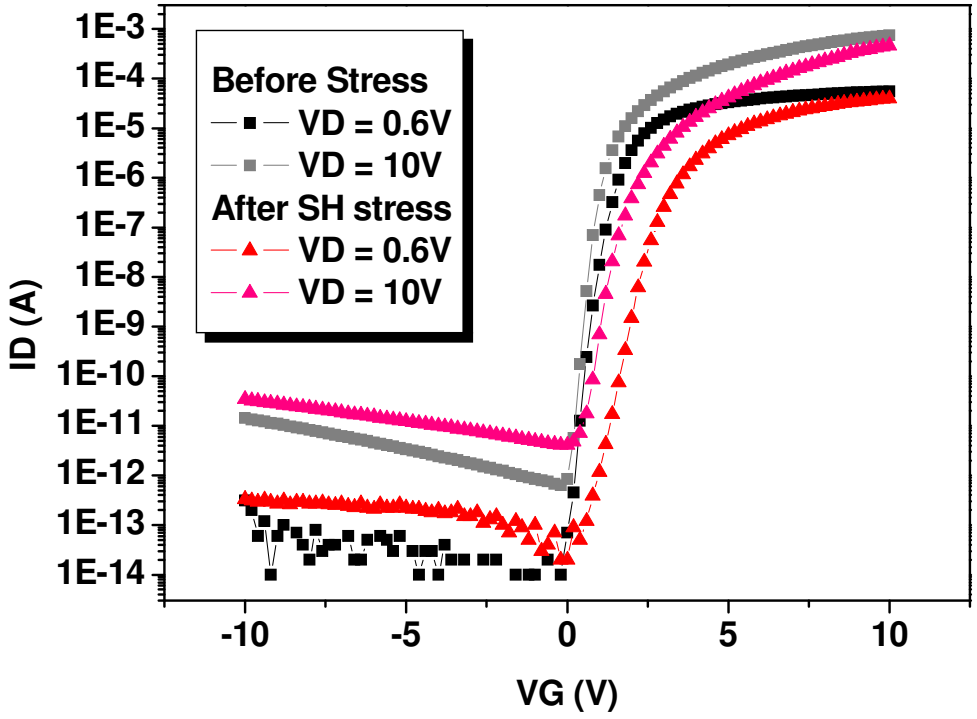

Fig. 4-12 IV curves before and after Self Heating stress.

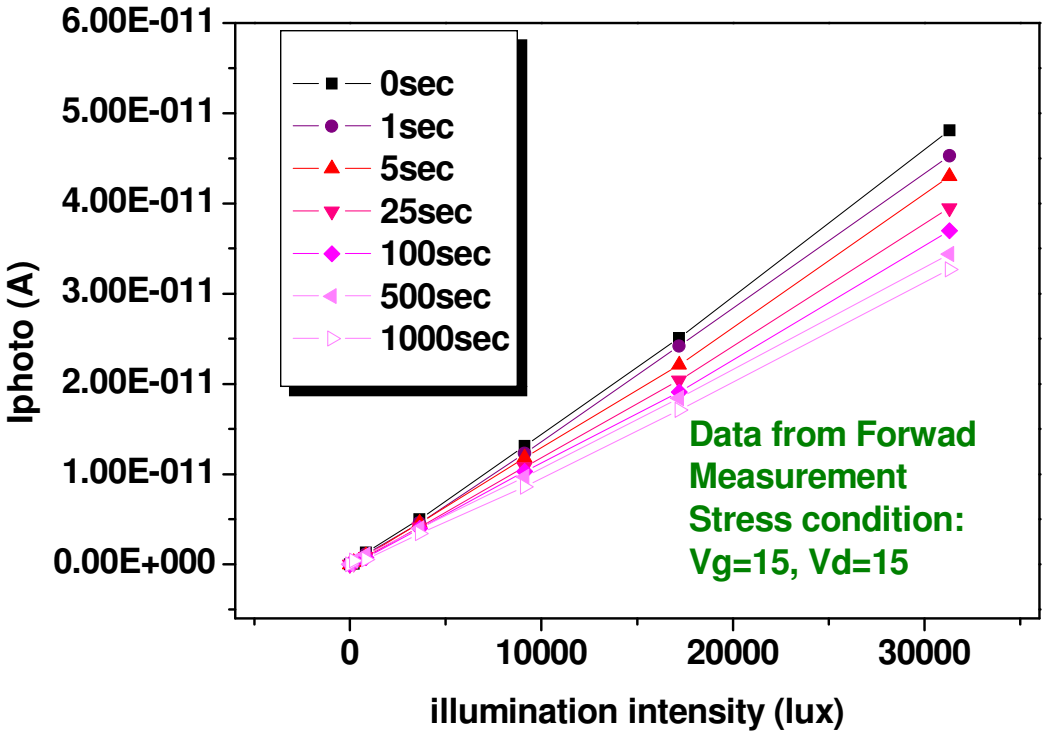

Fig.4-13(a) Photo current after Self Heating stress with different stress time(Forward).

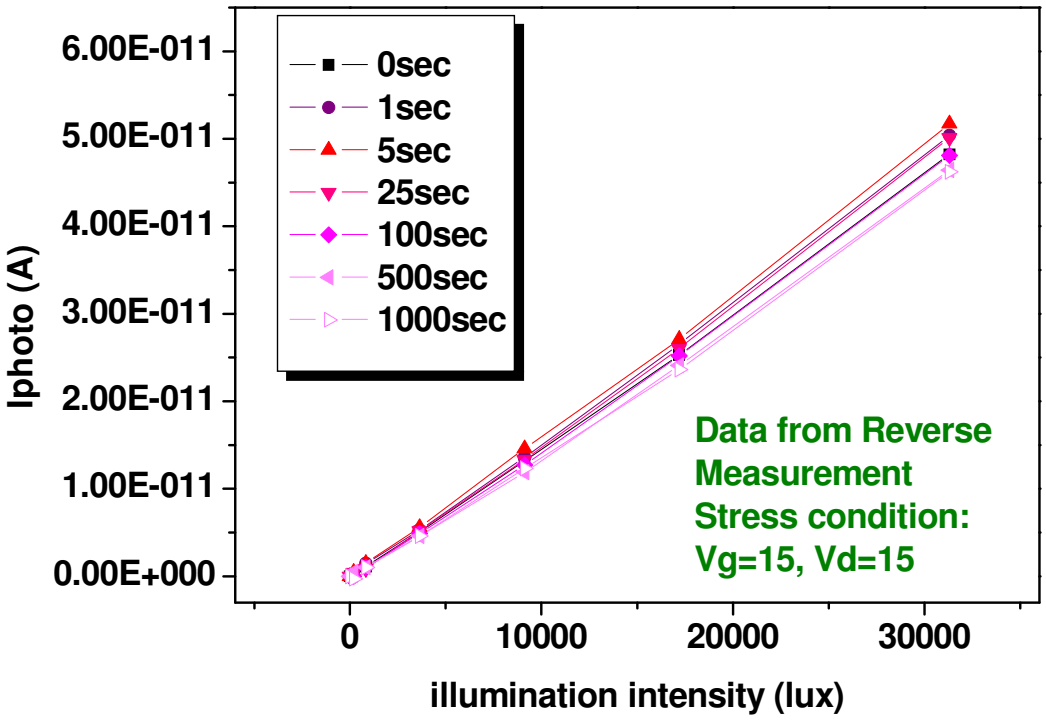

Fig.4-13(b) Photo current after Self Heating stress with different stress time(Reverse).

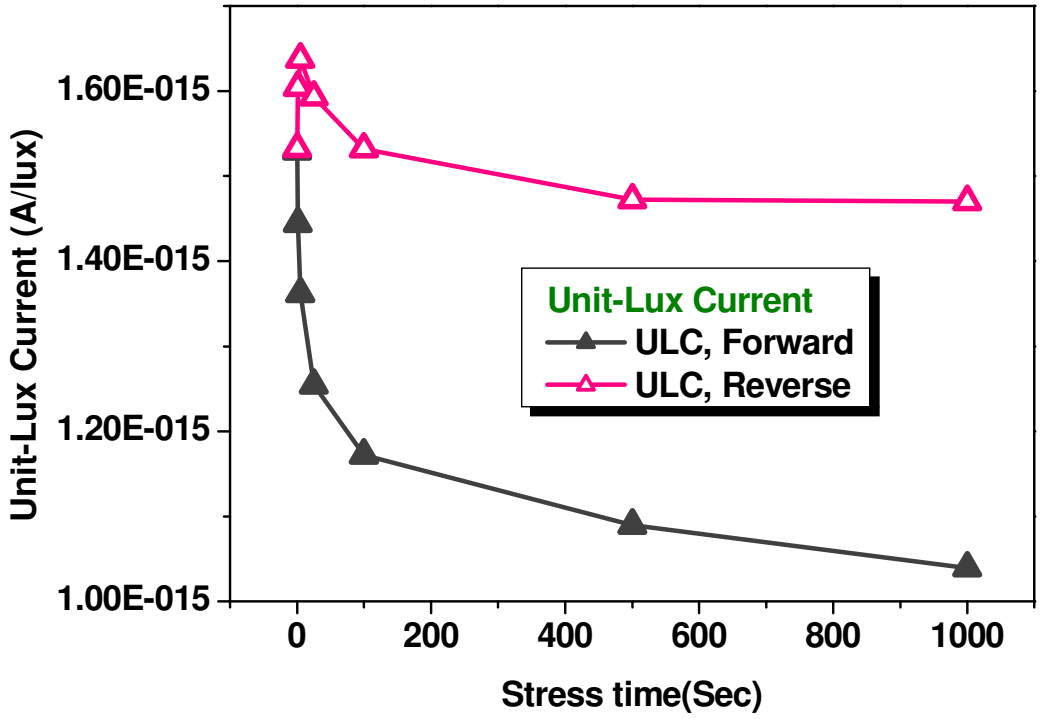

Fig. 4-14 Unit-Lux Current at (VD, VG) = (10V, -5V) with different stress time.

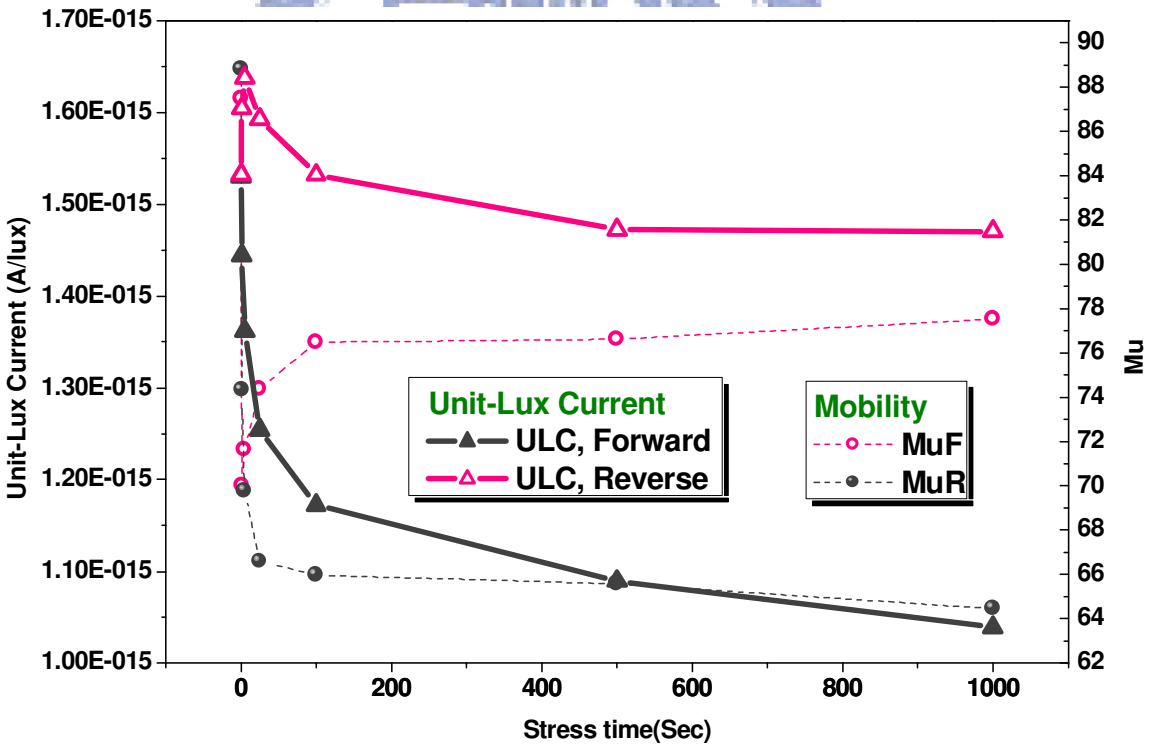

Fig. 4-15 (a) Variation trends of M μ and Unit-Lux Current with different stress time.

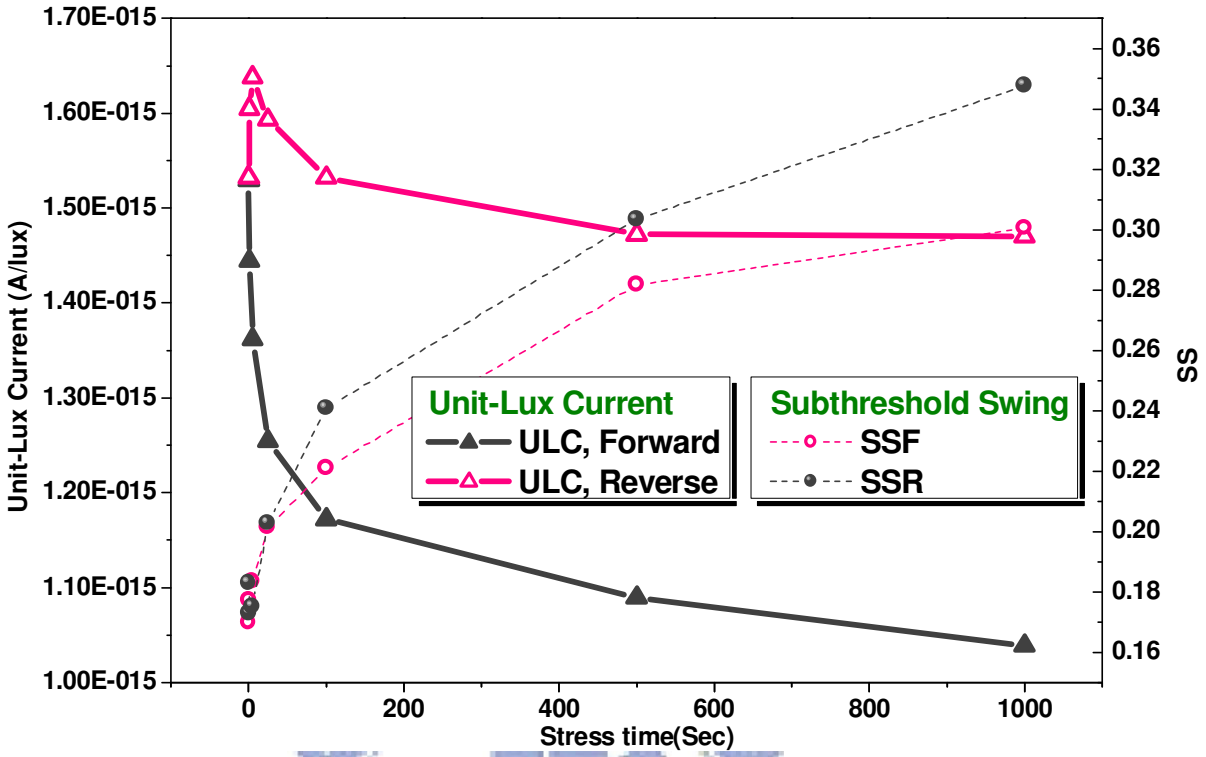

Fig. 4-15 (b) Variation trends of SS and Unit-Lux Current with different stress time.

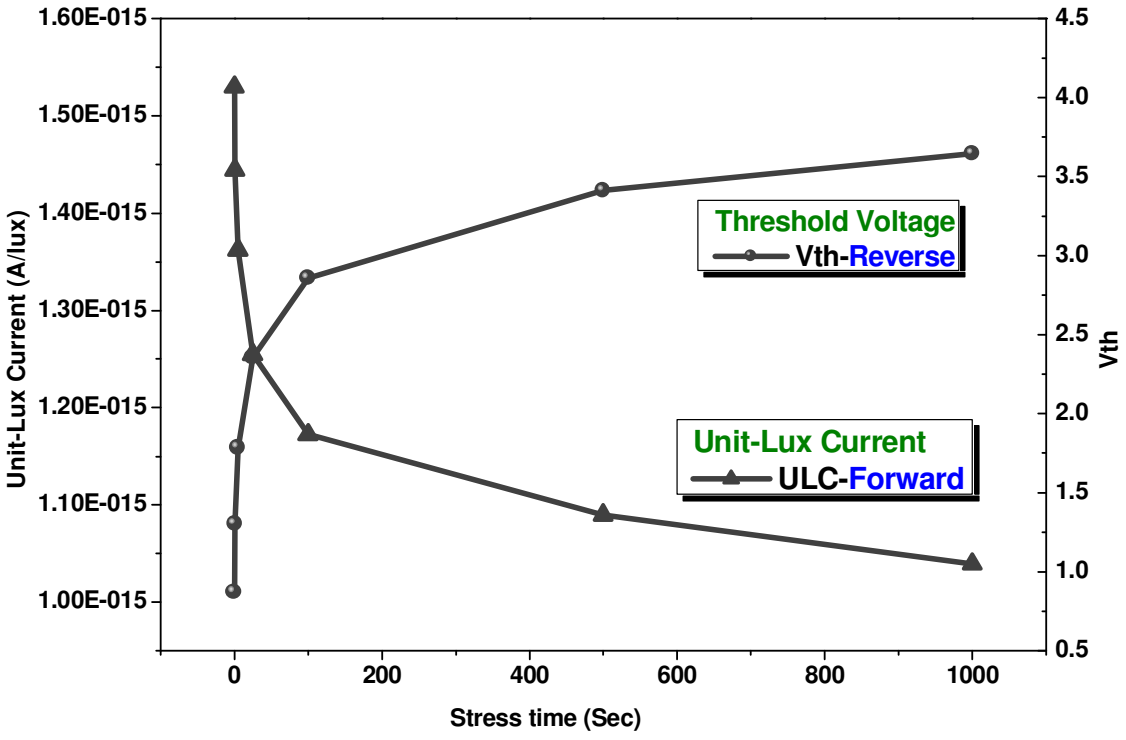

Fig. 4-16 (a) Reverse measured Vth and forward measured Unit-Lux Current.

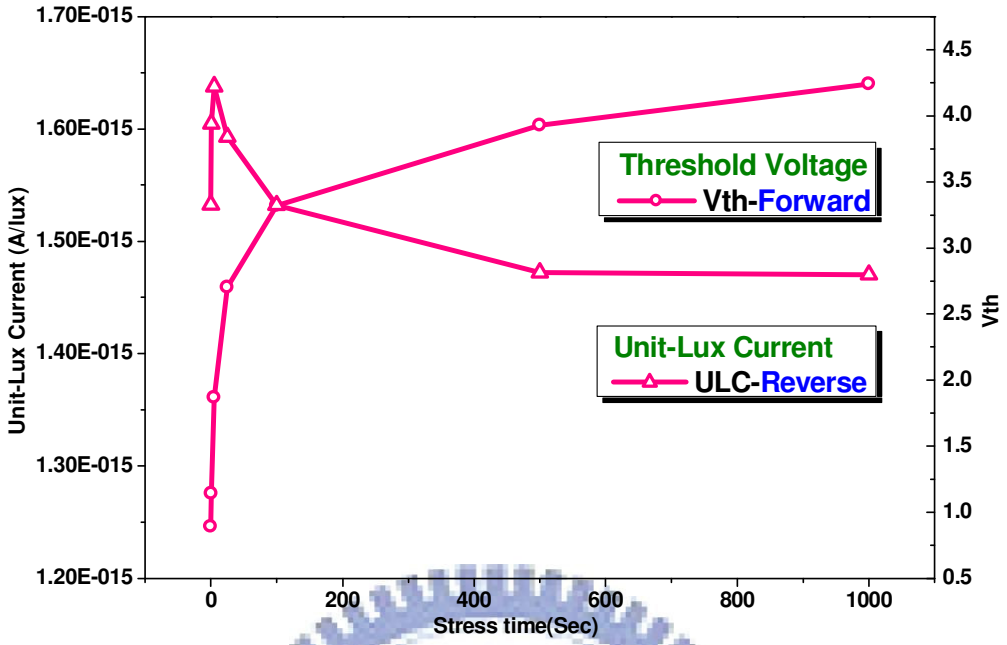

Fig. 4-16 (b) Forward measured Vth and reverse measured Unit-Lux Current.

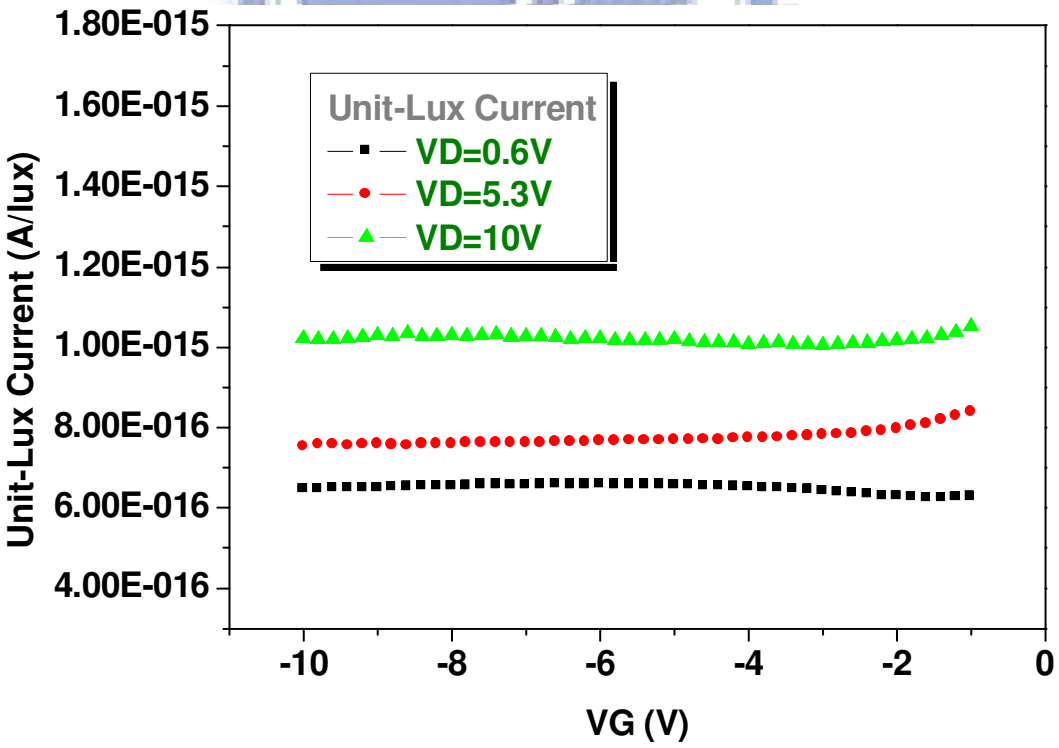

Fig. 4-17 (a) Gate bias dependence of Unit-Lux Current after Self Heating stress.

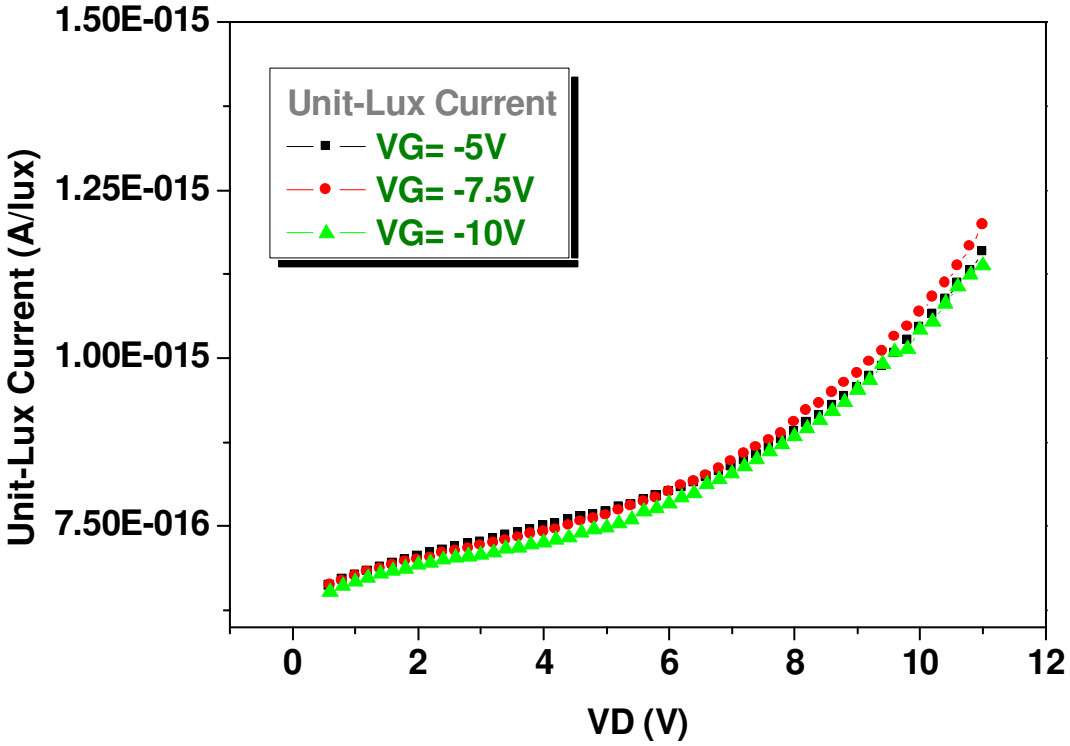

Fig. 4-17 (b) Drain bias dependence of Unit-Lux Current after Self Heating stress.

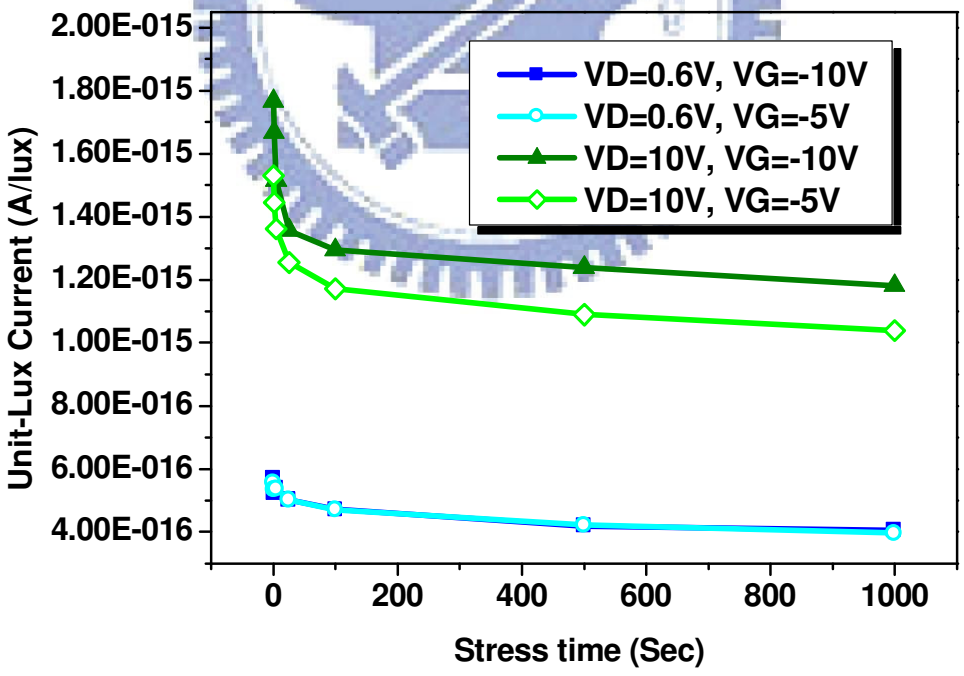

Fig. 4-18 Variation trends of Unit-Lux Current at different bias conditions.

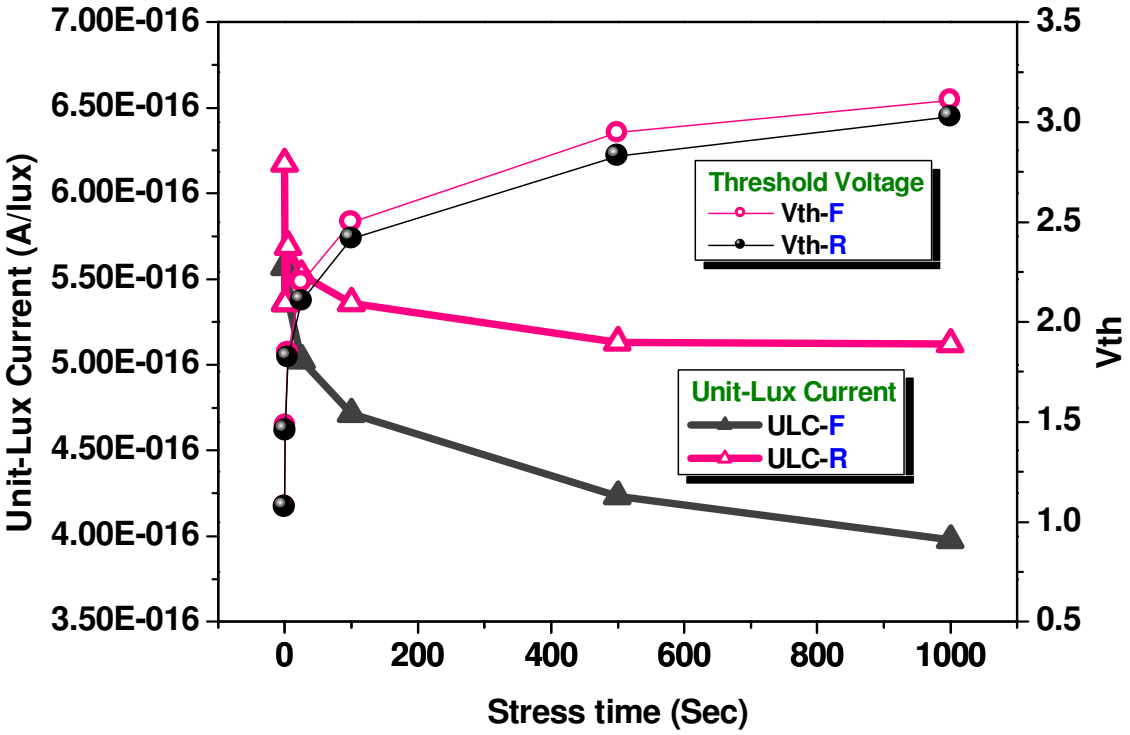

Fig. 4-19 Variation trends of Vth and Unit-Lux Current at VD = 0.6V.

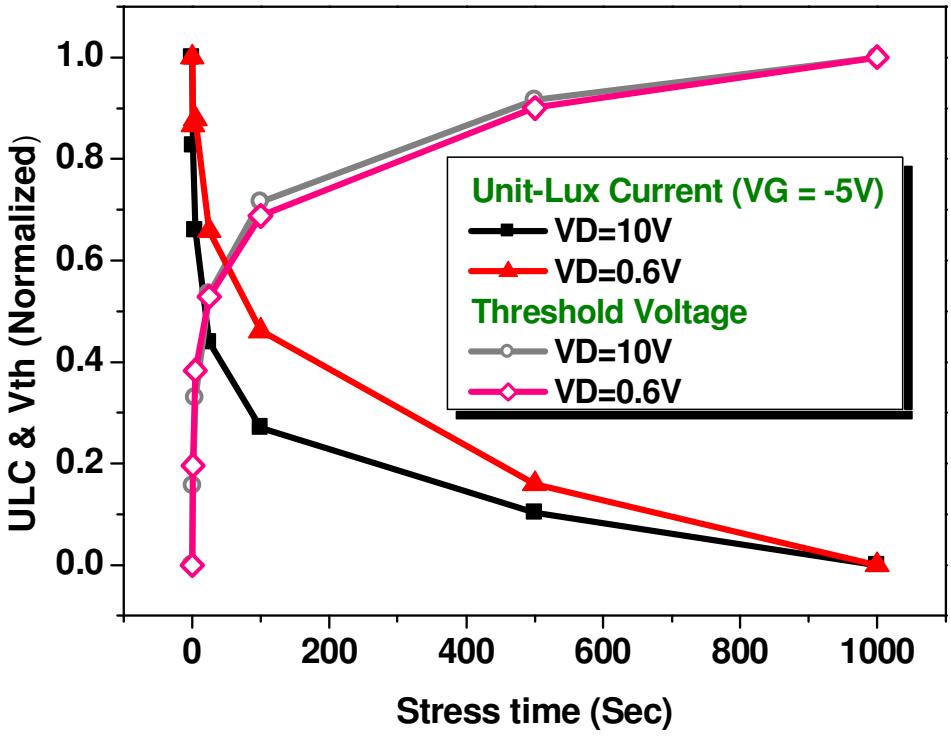

Fig. 4-20 Normalized Unit-Lux Current and Vth at VD = 10V and VD = 0.6V.

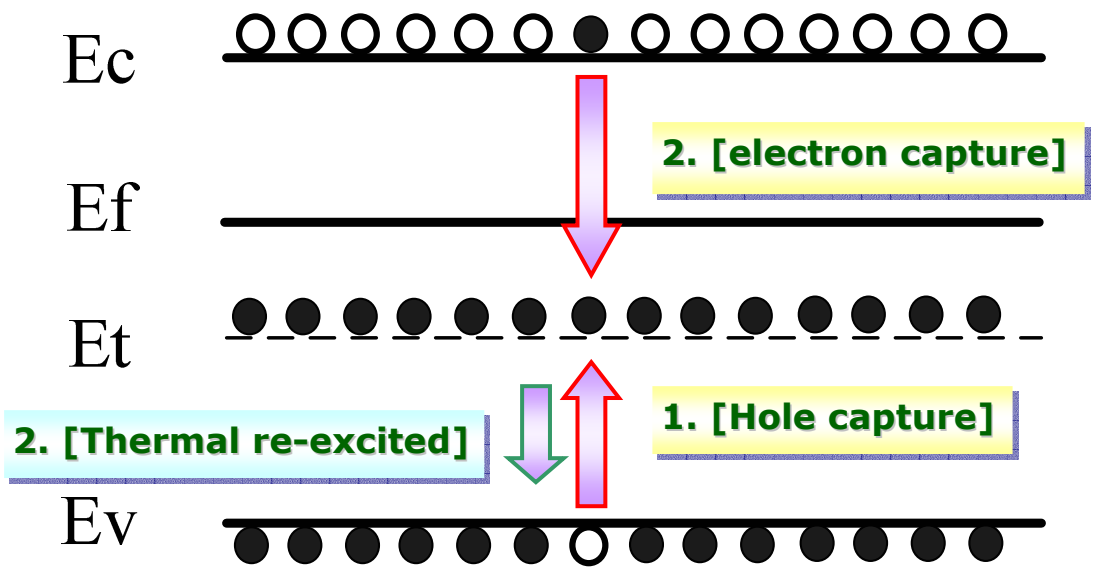

Fig. 4-21 Scheme of recombination process.

Chapter5

Conclusions

Effects of Temperature, electric field, and defect states in the energy gap on the photo leakage current of LTPS TFTs have been investigated. We can summarize several conclusions concisely:

The model of Unit-Lux Current has been developed. It can be expressed by a linear combination of two different terms. One of the terms called ULC_{C1} is proportional to the drain bias and increases with temperature exponentially. But it is independent of gate biases. ULC_{C1} may be induced by mechanisms like excess carrier diffusion or thermionic emission, thus it has strong dependence on temperature. The other component called ULC_{C2} is an exponential function of VD and VG. It is independent of temperature. ULC_{C2} is utterly an electric field dependent component thus we suppose that it is induced by mechanisms like excess carrier drift or field emission.

Different types of defect state result in distinct behaviors of the photo leakage current. Hot carrier stress creates tail state defects that enhance photo leakage current, and the increment of tail state defects can be reflected on the on-current mobility decrease. Self heating stress creates deep state defects that reduce photo leakage current, and the increment of deep state defects is reflected on the Threshold-Voltage increase.

REFERENCE

[1]. K . R. Olasupo and M. K. Hatalis, “Leakage current mechanism in sub-micron polysilicon thin-film transistors,” IEEE Trans. Electron Devices, Vol. 43, no. 8, pp. 1218–1223, Aug. 1996.

[2]. M. Yazaki, S. Takenaka, and H. Oshima, “Conduction mechanism of leakage current observed in metal-oxide-semiconductor transistors and poly-Si thin film transistors,” Jpn. J. Appl. Phys., Vol. 31, pp. 206-209, 1992.

[3]. K. Kobayashi, and Y. Niwano, “Photo-Leakage Current of Poly-Si Thin Film Transistors with Offset and Lightly Doped Drain Structure,” Jpn. J. Appl. Phys., Vol. 38, pp. 5757-5761, 1999.

[4]. K. Suzuki, F. Takeuchi, Y. Ebiko, M. Chida, and N. Sasaki, “Analytical Photo Leak Current model of Low-Temperature CW Laser Lateral Crystallization (CLC) Poly-Si TFTs,” Electron Devices Meeting, IEDM Technical Digest. IEEE International, pp.785- 788, 2004.

[5]. J. D. Gallezot, S. Martin and J. Kanicki, “Photosensitivity of a-si:H TFTs,” IDW, pp. 407-410, 2001.

[6]. Y. Uraoka, T. Hatayama, T. Fuyuki, T. Kawamura and Y. Tsuchihashi, “Hot Carrier Effects in Low-Temperature Polysilicon Thin-Film Transistors,” Jpn. J. Appl. Phys., Vol. 40, pp. 2833-2836, 2006.

[7]. S. Inoue, H. Ohshima and T. Shimoda, “Analysis of Degradation Phenomenon Caused by Self-Heating in Low-Temperature-Processed Polycrystalline Silicon Thin Film Transistors,” Jpn. J. Appl. Phys., Vol. 41 pp. 6313-6319, Nov 2002.

[8]. J. R. Ayres, S. D. Brotherton, I. R. Clarence and P. J. Dobson, “Photocurrents in poly-si TFTs,” IEE Proc.-Circuits Devices Syst. ,Vol. 141, No.1, February 1994.

[9]. S. Koide, S. Fujita, T. Ito, S Fujikawa, and T. Matsumoto, “LTPS Ambient Light Sensor with Temperature Compensation,” IDW, pp. 689-690, 2006.

[10]. N. P. Papadopoulos, A. A. Hatzopoulos, D. K. Papakostas, C. A. Dimitriadis, and S. Siskos, “Modeling the impact of light on the performance of polycrystalline thin-film transistors at the sub-threshold region,” Microelectronics Journal 37 (2006), 1313-1320.

[11]. Ya-Hsiang Tai, Shih-Che Huang, Chien-Wen Lin, and Hao Lin Chiu, “Degradation of the Capacitance-Voltage Behaviors of the Low-Temperature Polysilicon TFTs under DC stress,” Journal of The Electrochemical Society, 154 (7) H611-H618, 2007.

[12]. T. M. Brown ,and P. Migliorato, “Determination of the concentration of Hot carrier induced bulk defects in laser-crystallized polysilicon thin film transistors,” Appl. Phys. Lett., Vol. 76, p. 1024, 2000.

[13]. A. Valletta, L. Mariucci, and G. Fortunato, “Hot-Carrier-Induced Degradation of LDD polysilicon TFTs,” IEEE Transactions on Electron Devices, Vol. 53, No.1, pp. 43-50, January 2006.

[14]. S. Inoue, S. Takaneka, and T. Shimoda, “Study of Degradation Phenomenon Due to a Combination of Contamination and Self-Heating in Poly-si Thin Film Transistors Fabricated by a Low-Temperature Process,” Jpn. J. Appl. Phys., Vol.42, pp. 4213-4217, Part 1, No.7A, July 2003.

[15]. Y. Uraoka, K. Kitajima, H. Yano, T. Hatayama, T. Fuyuki, S. Hashimoto and Y. Morita, “Degradation of Low Temperature Poly-Si TFTs by Joule Heating,” proc. AMLCD 04, pp. 337-340.

[16]. T. Fuyuki, K. Kitajima, H. Yano, T. Hatayama, Y. Uraoka, S. Hashimoto, and Y. Morita, “Thermal degradation of low temperature poly-si TFT,” Thin solid Films 487 (2005), pp. 216-220.